

## Nuclear Quadrupole Interactions in Solids

By J. A. S. Smith

CHEMISTRY DEPARTMENT, KING'S COLLEGE,  
CAMPDEN HILL ROAD, LONDON W8 7AH

### 1 Introduction

The subject matter of this review begins on March 2nd, 1935 when H. Schüler and T. Schmidt at Potsdam submitted an article<sup>1</sup> to the *Zeitschrift für Physik* showing that the spacings of certain of the hyperfine lines in the atomic spectrum of the two europium isotopes <sup>151</sup>Eu and <sup>153</sup>Eu did not follow established rules (the Landé interval rule). To explain their results they proposed a new nuclear property, a deviation from spherical symmetry—a novel suggestion because until this date the nucleus of the Rutherford–Bohr atom had been imagined to be a very small sphere of roughly definable radius. This nuclear deformation involved a distortion from electrical symmetry, to which in a later paper the same authors gave the name 'quadrupole', following a suggestion by Delbrück.<sup>2</sup> The theoretical analysis of these observations followed quickly from H. B. G. Casimir,<sup>3</sup> who a year later published a summary of his work as a famous prize-winning essay now available as a book.<sup>4</sup> This group of papers laid the foundations of the subject matter of this review; they illustrate very clearly the strong connections between quadrupole interactions and atomic and later molecular spectroscopy on the one hand, and nuclear physics on the other. The spin quantum number and electric quadrupole moment of a nucleus are important properties for the study of nuclear deformations, a fortunate circumstance for the development of the chemical aspects of the subject, because of the effort that has subsequently been devoted to their reliable measurement.

The detection of quadrupole splittings in solids had to wait for another decade: in 1950 Pound<sup>5</sup> reported measurements of the <sup>23</sup>Na quadrupole splitting in a single crystal of NaNO<sub>3</sub> and in the same year Dehmelt and Krüger<sup>6</sup> published their observation of <sup>35</sup>Cl quadrupole resonance signals in polycrystalline *trans*-dichloroethylene. As in atoms, the frequencies observed depended on the electric field gradient at the nucleus, and provided thereby a sensitive probe of the electronic charge distribution. The way was now open for their study in solids by the techniques of magnetic resonance spectroscopy. The principal objective of such investigations, the elucidation of electronic structure and molecular motion in the solid state, is the subject matter of this review.

<sup>1</sup> H. Schüler and T. Schmidt, *Z. Phys.*, 1935, **94**, 457.

<sup>2</sup> H. Schüler and T. Schmidt, *Z. Phys.*, 1935, **95**, 265.

<sup>3</sup> H. B. G. Casimir, *Physica*, 1935, **2**, 719.

<sup>4</sup> H. B. G. Casimir, 'On the Interaction between Atomic Nuclei and Electrons', W. H. Freeman, San Francisco and London, 1963.

<sup>5</sup> R. V. Pound, *Phys. Rev.*, 1950, **79**, 685.

<sup>6</sup> H. G. Dehmelt and H. Krüger, *Naturwissenschaften*, 1950, **37**, 111.

## 2 The Quadrupole Coupling Constant

The discrepancies in the Eu spectra were explained by Casimir in terms of an interaction between the electric quadrupole moment of the nucleus,  $Q$ , of spin  $I$ , and the electric field gradient produced by the surrounding electrons,  $q$ ; their product  $e^2qQ/h$  in units of Hz, is generally referred to as the quadrupole coupling constant. The origin of this interaction is illustrated in Figure 1, in which the electric field gradient is generated by point positive charges. If a quadrupole is represented as two adjacent but antiparallel electric dipoles, it is clear that the orientation of Figure 1(a) has a lower energy than that of 1(b) and will therefore be preferentially adopted. Since all quadrupolar nuclei also have a magnetic moment, this ordering produces a magnetic polarization in a crystal, in a very similar way to that produced by a magnetic field.

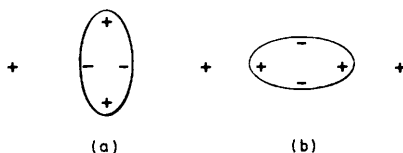


**Figure 1** Two orientations for an electric quadrupole moment in the electric field gradient of a point positive charge

The electric quadrupole moment is an intrinsic nuclear property<sup>7</sup> which can be measured, for example, by nuclear inelastic scattering; in the spectroscopic experiments to be discussed in this article, however, it is the value averaged over the spin motion of the nucleus that is observed, a quantity known as the 'spectroscopic' quadrupole moment. Such a moment is defined with respect to the axis,  $Oz$ , of nuclear spin and the nuclear charge distribution which generates it must therefore have cylindrical symmetry about this axis. Two such common distributions then arise; in the first, a spherical charge distribution is compressed along the direction,  $Oz$ , of nuclear spin, to give a tangerine-shaped object, or an oblate spheroid; in the second, the sphere is extended along the direction  $Oz$ , to give a rugby-football-shaped object, or a prolate spheroid (as in Figure 1). If  $e\rho_n$  is the nuclear charge density (taken as positive), the quadrupole moment of such charge distributions may be defined by the equation ( $-e$  is the charge on the electron)

$$eQ = e \int \rho_n (3z^2 - r^2) dr \quad (1)$$

for a nucleus in the spin state  $m_1 = I$  ( $m_1$  being the nuclear magnetic quantum number). It will be seen that  $Q$  defined in this way has dimensions of length<sup>2</sup> and in the SI system units of m<sup>2</sup>, and is positive for prolate and negative for oblate spheroids.  $Q$  varies periodically in both sign and magnitude as the nuclear charge increases due to the effect of nuclear shell structure, there being zeroes at the 'magic numbers' of like nucleons 2,8,20,28,50,82,126; the maximum and minimum values

<sup>7</sup> P. Brix, *Z. Naturforsch. A.* 1986, 41 to be published.

increase in magnitude as  $Z$  increases and there tend to be more nuclei with positive  $Q$  than with negative  $Q$ . In magnitude, it is of the order of nuclear cross-sections, *i.e.*  $(10^{-14})^2$  or  $10^{-28}$  m<sup>2</sup> which is called one 'barn' and is equal to 100 fm<sup>2</sup>. So for  ${}^2\text{H}$ ,  $Q$  is close to  $+0.286$  fm<sup>2</sup> (or 2.86 mb) whereas for a heavy nucleus<sup>8</sup> such as  ${}^{223}\text{Ra}$  it rises to 120 fm<sup>2</sup>. An important condition<sup>9</sup> imposed by the symmetry properties of the nucleus on the spectroscopic quadrupole moment is that it is only non-zero if the nuclear spin quantum number  $I \geq 1$  so  ${}^1\text{H}$  ( $I = \frac{1}{2}$ ) is non-quadrupolar, but  ${}^2\text{H}$  ( $I = 1$ ) is. The number of atomic nuclei in the Periodic Table which are both reasonably abundant and quadrupolar is about fifty.

The electric field gradient,  $q$ , at a nuclear site arises from the electronic charge distribution in atoms, and from both electrons and neighbouring nuclei in molecules. It is zero for electrons in  $s$ -orbitals, which because of their spherical symmetry cannot generate an electric field gradient; the non-zero value of the  $s$ -electron density over the finite nuclear volume does not affect this argument, since the corresponding energy of interaction is independent of nuclear orientation. It is zero at sites of  $T_d$  and  $O_h$  symmetry in rigid molecules. We therefore consider the case of an electron in a  $p$ -orbital, which can generate an electric field gradient; consider a volume element  $d\tau$  of electronic charge density  $\rho_e$  in Coulombs m<sup>-3</sup>, including sign, distance  $r$  from the nucleus placed at the origin, with Cartesian coordinates  $(x,y,z)$  (Figure 2). The electrostatic potential produced by this volume element at the origin is

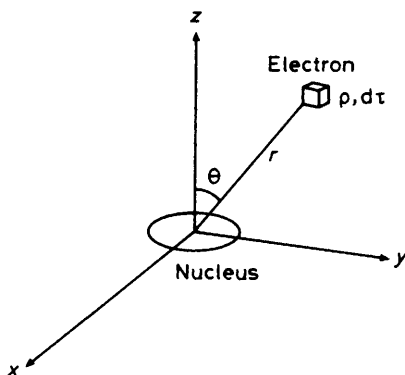


**Figure 2** A volume element,  $d\tau$ , of electronic charge density,  $\rho_e$ , distance  $r$  from the nucleus at the origin

$$V = \rho_e \frac{d\tau}{r} \quad (2)$$

The electric field along  $Oz$  is thus an integral over the charge distribution

<sup>8</sup> S. A. Ahmad, W. Klempt, R. Neugart, E. W. Otten, K. Wendte, C. Ekström, and ISOLDE collaboration, *Phys. Lett. B*, 1983, **133**, 47.

<sup>9</sup> N. F. Ramsey, 'Nuclear Moments', Wiley, New York, 1953.

$$E_z = -\frac{\partial V}{\partial z} = \int \rho_e \left( \frac{z}{r^3} \right) d\tau = \int \rho_e \frac{\cos\theta}{r^2} d\tau \quad (3)$$

since  $dr/dz = z/r = \cos\theta$ ,  $\theta$  being the polar angle (Figure 2). Hence the second derivative of  $V$  or the first derivative of  $E_z$ , the electric field along  $Oz$ , is

$$eq_{zz} = V_{zz} = \frac{\partial^2 V}{\partial z^2} = \int \rho_e \left( \frac{3\cos^2\theta - 1}{r^3} \right) d\tau \quad (4)$$

The quantity  $q_{zz}$  is often loosely referred to as the electric field gradient—it is in fact the negative of this quantity, as equations (3) and (4) reveal. Two other components may also be derived

$$\begin{aligned} eq_{xx} &= V_{xx} = \frac{\partial^2 V}{\partial x^2} = \int \rho_e \left( \frac{3\sin^2\theta\cos^2\varphi - 1}{r^3} \right) d\tau \\ eq_{yy} &= V_{yy} = \frac{\partial^2 V}{\partial y^2} = \int \rho_e \left( \frac{3\sin^2\theta\sin^2\varphi - 1}{r^3} \right) d\tau \end{aligned} \quad (5)$$

and there are also cross-derivatives such as  $\partial^2 V/\partial x\partial y$ , nine in total. The electric field gradient defined in this way is thus a *tensor* of second rank, in this case symmetric, since  $\partial^2 V/\partial y\partial x = \partial^2 V/\partial x\partial y$  and traceless since from equations 4 and 5

$$q_{xx} + q_{yy} + q_{zz} = 0 \quad (6)$$

which is simply a statement of Laplace's equation in electrostatics. These equations are valid for an atom; for a molecule, we must in addition consider the contribution of adjacent nuclei, considered as point charges  $Z_i e$  distance  $R_i$  from the nucleus in question. Hence the total electric field gradient at a given nuclear site with respect to axes embedded in the molecule is

$$V_{zz} = eq_{zz} = -e \int_{\text{electrons}} \psi^* \left( \frac{3\cos^2\theta - 1}{r^3} \right) \psi d\tau + \sum_{\text{nuclei}} Z_i e \left( \frac{3\cos^2\theta_i - 1}{R_i^3} \right) \quad (7)$$

in which the electronic charge density has been replaced by the product  $\psi^*\psi$  of the electronic wave functions (note that  $e$  in equation 7 is un-signed). There will be similar expressions to equation 7 for  $q_{yy}$ ,  $q_{xx}$ , . . . *etc.*; we now use a characteristic property of tensors<sup>10</sup> that it is always possible to find a set of axes, known as the principal axes, in which the cross-derivatives  $\partial^2 V/\partial x\partial y$  *etc.* are zero and only  $q_{xx}$ ,  $q_{yy}$ , and  $q_{zz}$  finite. From henceforth these quantities will denote the principal components and we use the common convention that

$$|q_{zz}| \geq |q_{yy}| \geq |q_{xx}| \quad (8)$$

so that  $q_{zz}$  is the largest (in magnitude) of the three principal components of the electric field gradient. It is customary to set

<sup>10</sup> J. F. Nye. *Physical Properties of Crystals*, Clarendon Press, Oxford, 2nd Edition, 1985.

$$q_{zz} = q \quad (9)$$

which is the quantity that appears in the definition of the quadrupole coupling constant,  $e^2qQ/h$ .

In atoms,  $q_{xx} = q_{yy} = -\frac{1}{2}q_{zz}$  from equation 6; in molecules, this is not necessarily the case unless the nucleus lies on a threefold (or higher) symmetry axis of the molecule coincident with the direction of  $q_{zz}$ . Since only *two* components of  $q$  are truly independent, it is usual to define an asymmetry parameter  $\eta$  by the equation

$$\eta = (q_{xx} - q_{yy})/q_{zz} \quad (10)$$

which from equations 6 and 8 will be a positive number lying between 0 and 1. The quadrupole interaction in a molecule is therefore defined in the general case by five quantities; the quadrupole coupling constant ( $e^2qQ/h$ ), the asymmetry parameter  $\eta$ , and the directions of the three principal axes of the electric field gradient tensor with respect to axes fixed in the molecule. Note that  $e^2qQ/h$  has a sign:  $Q$  does and  $q_{zz}$  has according to which term on the right hand side of equation 7 dominates, and so therefore does their product.

In almost all the experiments to be discussed in this article, it is the product of  $q$  and  $Q$  that is derived experimentally. Admittedly, the quadrupole interaction for the same nucleus may be measured in a wide range of compounds, by methods to be surveyed in the next section, so that relative values of  $q$  can be compared; nevertheless, in order to relate them to some quantitative feature of the electron distribution, an estimate of absolute values needs to be made, and this requires a knowledge of the nuclear quadrupole moment. There would, at first sight, appear to be no problem. One could take an ion-pair such as  $^{39}\text{K} + ^{35}\text{Cl}^-$  or  $^{39}\text{K} + ^{37}\text{Cl}^-$  in the gas phase, where both nuclei  $^{39}\text{K}$  ( $I = \frac{3}{2}$ ) and  $^{35,37}\text{Cl}$  ( $I = \frac{3}{2}$ ) are quadrupolar and where their quadrupole coupling constants are known from electric beam resonance methods ( $\eta = 0$  in this case),<sup>11</sup> evaluate the electric field gradient at one nucleus due to the charge on the neighbouring ion by inserting the known internuclear distance into equation 4 (taking  $\cos\theta = 1$ ), and so derive  $Q$ . Allowance could be made for the finite size of the ions and their polarizability. As Casimir realized, such simple methods are bound to fail because of deformations of the electron core caused by the electric field gradient and nuclear quadrupole moment. The result in most negative ions is anti-shielding—the quadrupolar distortion of the inner shells produces a much larger interaction with an external electric field gradient than that which would be observed for a ‘bare’ nucleus; since the problem was first treated quantitatively by Sternheimer,<sup>12</sup> the factor is known as the Sternheimer factor and given the symbol  $\gamma$ . The origin of these effects is illustrated in Figure 3: a spherical shell of charge surrounding the nucleus is distorted by the electric quadrupole moment of the latter in two ways, a radial distortion in which negative charge is repelled radially from A and B and attracted at C and D, and an

<sup>11</sup> N. F. Ramsey, ‘Molecular Beams’, Clarendon Press, Oxford, 1956, Chapter XI.

<sup>12</sup> R. Sternheimer, *Phys. Rev.*, 1950, **80**, 102; 1951, **84**, 244; 1952, **86**, 316; 1954, **95**, 736, and later papers.

angular distortion in which charge is moved within the shell from A to D or C and B to C or D. By means of the latter, an electron in an  $s$ -orbital acquires a little of the appearance of a  $d$ -orbital, so these distortions are often called excitations and represented by  $ns \rightarrow d$ , etc. Both effects must be allowed for in any calculation; Sternheimer also showed that this distortion is equal to that which would be calculated if we had allowed the external electric field gradient to distort the charge distribution of the atom in question, which then interacts with the electric quadrupole moment of the nucleus. The result of these two interactions is to add an extra term to the predicted electric field gradient,  $V_{zz}^0$ , in the absence of shielding, given by

$$V_{zz}^0(1 - \gamma) \tag{11}$$

Shielding corresponds to values of  $\gamma$  lying between 0 and 1 and antishielding corresponds to negative values of  $\gamma$ , which can be very large for highly polarizable negative ions such as  $I^-$  in which  $\gamma_\infty$  is  $-332$  (this quantity refers to the Sternheimer ionic antishielding factor for distant ions, with no core penetration).<sup>13</sup> For atoms, much smaller values are derived, e.g.  $(1 - \gamma) = 0.830$  in  ${}^7\text{Li}$  derived from a calculation using many-body perturbation theory, the result corresponding to shielding.<sup>14</sup> Even with calculations of this degree of rigour, the derivation of a reliable value of  $Q$  still requires hyperfine data of high accuracy and resolution; between them, these two factors have until recently limited the accuracy of Sternheimer factors in atoms available in the literature. With new and more reliable values of hyperfine splittings coming from the study of fast ion beams by crossed or collinear beam laser spectroscopy,<sup>15</sup> in which the velocity spread in the beam and hence the line width are very considerably reduced, this situation is now changing.

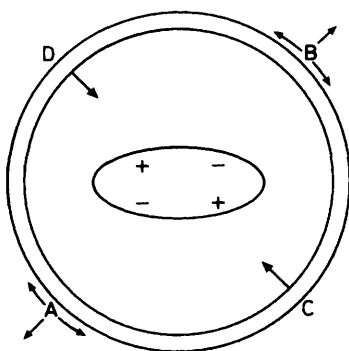


**Figure 3** *Origin of Sternheimer anti-shielding*

<sup>13</sup> K. D. Sen and P. T. Narasimhan, *Adv. Nucl. Quad. Res.*, 1974, **1**, 277.

<sup>14</sup> J. D. Lyons, R. T. Pu, and T. P. Das, *Phys. Rev.*, 1969, **178**, 103.

<sup>15</sup> E. W. Otten, *Hyperfine Interactions*, 1985, **21**, 43.

An alternative approach is to make absolute measurements of  $Q$ , free from Sternheimer corrections. One technique is to study nuclear–nuclear scattering in a Coulomb field (*i.e.* outside the nuclear forces) for which the quadrupole contribution can be accurately calculated. Thus the angular variation in the scattering of a beam of aligned  ${}^7\text{Li}^{3+}$  ions at Ni or Sn targets has been analysed, and from the ratios of the differential scattering cross-sections for unpolarized and aligned  ${}^7\text{Li}$  beams a value of  $Q({}^7\text{Li}) = -3.70(8) \text{ fm}^2$  has been deduced.<sup>16</sup> The method, unfortunately, is restricted to the lightest atoms. For heavier nuclei, the hyperfine splitting of ‘muonic’ atoms has been analysed. Such atoms are produced by negative muon capture by the nucleus of the atom under study; if the muon enters an orbit which lies outside the nucleus but well within the inner electron shells, then the latter exert no shielding or antishielding effect. Such muonic atoms show ‘atom-like’ spectra with a hyperfine structure dominated by the quadrupole moment of the ‘bare’ nucleus. Thus muonic  ${}^{23}\text{Na}$  gives a resolvable hyperfine structure for the  $3d_{\frac{3}{2}} - 2p_{\frac{3}{2}}$  transition<sup>17</sup> due largely to the hyperfine interaction in the  $2p_{\frac{3}{2}}$  state, from which a value of  $Q({}^{23}\text{Na}) = +10.06(20) \text{ fm}^2$  can be determined. The same technique has been used to study  ${}^{25}\text{Mg}$  [ $Q = +20.1(3) \text{ fm}^2$ ] and  ${}^{27}\text{Al}$  [ $Q = 15.0(6) \text{ fm}^2$ ], and applied to the study of muonic M or N X-rays from heavier atoms<sup>18</sup> such as  ${}^{151}\text{Eu}$  [ $Q = 90.3(10) \text{ fm}^2$ ] and even as high as  ${}^{233}\text{U}$  [ $Q = +366.3(8) \text{ fm}^2$ ] and  ${}^{235}\text{U}$  [ $Q = 493.6(6) \text{ fm}^2$ ]. The muonic orbits must be large enough to avoid significant nuclear deformation; even then, small corrections may be necessary to allow for overlap of the muon with the nuclear charge density. Despite these problems, the method is likely to be of increasing importance.

### 3 The Measurements of Quadrupole Interactions in Solids

Quadrupole interactions can be measured in the gas, liquid, and solid states: in the gas by high-resolution atomic spectroscopy, as already mentioned at the end of the previous section, or molecular microwave spectroscopy,<sup>19</sup> and in liquids by studying solutions in oriented mesophases<sup>20</sup> or the high resolution nuclear magnetic resonance spectra of molecules partially aligned by means of their magnetic anisotropy or polar molecules by application of an external electric field.<sup>21</sup> This review, however, is largely confined to solid state measurements, in which the quadrupole resonance interactions can be measured directly, even in powders, and without any magnetic field. To understand how this possibility arises, it is necessary to derive the energy of interaction of a nuclear electric quadrupole moment in the electric field gradient of an external charge distribution—the so-

<sup>16</sup> A. Weller, P. Egelhof, R. Čaplar, O. Karban, D. Krämer, K.-H. Möbius, Z. Moroz, K. Rusek, E. Steffens, G. Taugate, K. Blatt, I. Koenig, and D. Fick, *Phys. Rev. Lett.*, 1985, **55**, 480.

<sup>17</sup> B. Jeckelman, W. Beer, I. Beltrami, F. W. N. de Boer, G. de Chambrier, P. F. A. Goudsmit, J. Kern, J. J. Leisi, W. Ruckstuhl, and A. Vacchi, *Nucl. Phys. A*, 1983, **408**, 495.

<sup>18</sup> Y. Tanaka, R. M. Steffen, E. B. Shera, W. Reuter, M. V. Hoehn, and J. D. Zumbro, *Phys. Rev. Lett.*, 1983, **51**, 1633.

<sup>19</sup> W. Gordy and R. L. Cook, ‘Microwave Molecular Spectra’, Wiley, New York, 3rd Edition, 1984.

<sup>20</sup> A. Loewenstein, *Adv. Nucl. Quad. Res.*, 1983, **5**, 53.

<sup>21</sup> P. C. M. Van Zijl, B. H. Ruessink, J. Bulthuis, and C. MacLean, *Acc. Chem. Res.*, 1984, **17**, 172.

called quadrupolar Hamiltonian. This derivation is discussed in detail by Slichter<sup>22</sup> and the interested reader is referred to this excellent text. We quote here the result: in the principal-axis frame of reference, the energy operator  $\hat{H}_Q$  is

$$\hat{H}_Q = \frac{e^2qQ}{4I(2I-1)} \left\{ 3\hat{I}_z^2 - I(I+1) + \frac{\eta}{2} (\hat{I}_+^2 + \hat{I}_-^2) \right\} \quad (12)$$

in which  $\hat{I}_z$ ,  $\hat{I}_+$ , and  $\hat{I}_-$  are nuclear spin operators, the former corresponding to the  $z$ -component and the two latter to the raising and lowering operators expressed in terms of the  $x$  and  $y$  components by  $\hat{I}_\pm = \hat{I}_x \pm i\hat{I}_y$ . Operation on the appropriate nuclear spin eigenfunctions will then give the quadrupolar energy levels between which transitions occur according to the usual magnetic selection rule  $\Delta m_I = \pm 1$ .

The model of Larmor precession of a nuclear gyromagnet in a magnetic field, much used in nuclear magnetic resonance, has some parallel here. In the magnetic case, the nuclear moment responds to the turning torque tending to align it with the field by precessing about it at an angular frequency equal to  $\gamma H_0$ , where  $\gamma$  is the nuclear gyromagnetic ratio. In the quadrupolar case (Figure 1), the action of the turning torque tending to align the nuclear electric quadrupole moment in the electric field gradient produces quadrupole precession about the symmetry axis of the latter at an angular frequency  $\omega_Q$  proportional to the quadrupole coupling constant. This quadrupole precession is the classical analogue<sup>23</sup> of the transition frequency obtained by solution of equation 12, and is useful in providing a simple model for the transition. The precessional motion of the quadrupole carries the nuclear magnetic moment with it; a radiofrequency field  $H_1$  perpendicular to the symmetry axis and in synchronism with the angular frequency  $\omega_Q$  will couple to this moment, with which it can exchange energy, thus altering the angle of inclination of the electric quadrupole moment to the symmetry axis of the electric field gradient, and thereby changing its energy. We have therefore a close parallel to nuclear magnetic resonance absorption; in both, we study magnetic dipole transitions, for which the usual selection rule is  $\Delta m_I = \pm 1$ , but the origin of the splitting is different, in one case being electric, in the other magnetic. The concept of the 'rotating frame' can also be used, although the mathematical transformations are more complex than in the case of nuclear magnetic resonance;<sup>24</sup> sitting in a frame rotating at  $\omega_Q$  with the quadrupole precession 'removes' the effects of the latter and leaves only the influence of the radiofrequency field,  $H_1$ , about which the nucleus precesses at an angular frequency proportional to  $\gamma_Q H_1$ ,  $\gamma_Q$  being the gyromagnetic ratio of the quadrupolar nucleus.

The model we have been discussing is appropriate to what is often called 'pure' nuclear quadrupole resonance spectroscopy, in which transitions between the quadrupolar levels are directly excited by radiofrequency radiation of the correct frequency, in zero magnetic field. The term is not altogether satisfactory; we are

<sup>22</sup> C. P. Slichter, 'Principles of Magnetic Resonance', Springer-Verlag, Berlin-Heidelberg-New York, 2nd Edition, 1978, Chapter 9.

<sup>23</sup> J. C. Raich and R. H. Good Jr., *Am. J. Phys.*, 1963, 31, 356.

<sup>24</sup> A. Abragam, 'Principles of Nuclear Magnetism', Clarendon Press, Oxford, 1961.



really discussing a form of zero-field nuclear magnetic resonance spectroscopy, in which the level splitting is thoughtfully provided by Nature and not by a laboratory magnet. Nature, as usual, gives with one hand and takes away with the other; since we have little or no control over the electric field gradient, the nuclear quadrupole resonance frequencies can be anywhere in an enormous range, from a few kHz to a thousand MHz or more, depending on the magnitude of the nuclear electric quadrupole moment.

To return to the quantum-mechanical Hamiltonian, equation 12, the solutions obtained<sup>25</sup> depend on the nuclear spin quantum number  $I$ . For spin-1 nuclei, the actual eigenstates are linear combinations of the  $m_I$  sub-states  $+1, 0, -1$ , and are given by

$$\begin{aligned} y &= \frac{1}{\sqrt{2}}(|+1\rangle + |-1\rangle) & E_y &= \frac{1}{4}(e^2qQ)(1 + \eta) \\ x &= \frac{1}{\sqrt{2}}(|+1\rangle - |-1\rangle) & E_x &= \frac{1}{4}(e^2qQ)(1 - \eta) \\ z &= |0\rangle & E_z &= -\frac{1}{2}(e^2qQ) \end{aligned} \quad (13)$$

and three transitions are allowed (Figure 4) with frequencies

$$\begin{aligned} \nu_x(\nu_+) &= \frac{3}{4}(e^2qQ/h)(1 + \eta/3) \\ \nu_y(\nu_-) &= \frac{3}{4}(e^2qQ/h)(1 - \eta/3) \\ \nu_z(\nu_0) &= \frac{1}{2}(e^2qQ/h)\eta \end{aligned} \quad (14)$$

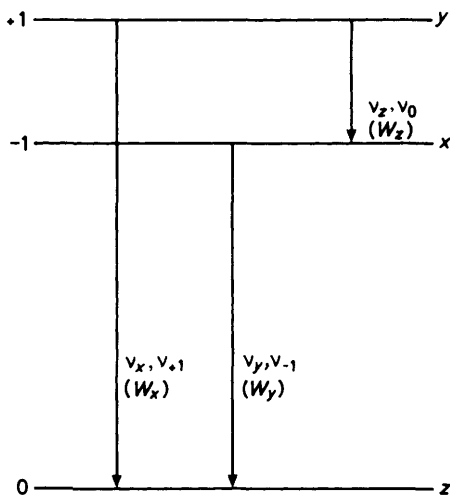


Figure 4 Energy level diagram for a spin-1 nucleus such as  $^{14}\text{N}$  or  $^2\text{H}$

which reduce to just one when  $\eta = 0$ . These equations give the two commonly used notations for the three frequencies; observation of any pair, correctly identified, will

<sup>25</sup> T. P. Das and E. L. Hahn, 'Nuclear Quadrupole Resonance Spectroscopy', Academic Press, New York and London, 1958.

lead to values for the quadrupole coupling constant and asymmetry parameter which can be checked if the third frequency is also detected. Such transitions can be observed not only in a single crystal but also in powders, since the quantization axis of the spins is internal to the sample and is not provided by any external agency. In powders, however, the directions of the principal axes and the sign of the quadrupole interaction are not usually derived from the experiment.

For half-integral spins, the eigenstates and energy levels occur in degenerate pairs, known as Kramers doublets since they arise as a consequence of Kramers theorem.<sup>26</sup> For  $I = \frac{3}{2}$  (e.g. <sup>7</sup>Li, <sup>35</sup>Cl, <sup>37</sup>Cl, <sup>79</sup>Br, <sup>81</sup>Br) the eigenstates once again are suitable linear combinations of the  $m_1$  sub-states  $+\frac{3}{2}$ ,  $+\frac{1}{2}$ ,  $-\frac{1}{2}$ ,  $-\frac{3}{2}$ ; two examples of the four possible combinations, with the corresponding energies, are

$$\Psi_{+\frac{3}{2}} = c_{-\frac{1}{2},\frac{3}{2}}|-\frac{1}{2}\rangle + c_{\frac{3}{2},\frac{3}{2}}|+\frac{3}{2}\rangle, \quad E_{\pm\frac{3}{2}} = \frac{1}{4}(e^2qQ)\left(1 + \frac{\eta^2}{3}\right)^{\frac{1}{2}} \quad (15)$$

$$\Psi_{+\frac{1}{2}} = c_{\frac{3}{2},\frac{1}{2}}|\frac{1}{2}\rangle + c_{-\frac{1}{2},\frac{1}{2}}|-\frac{3}{2}\rangle, \quad E_{\pm\frac{1}{2}} = -\frac{1}{4}(e^2qQ)\left(1 + \frac{\eta^2}{3}\right)^{\frac{1}{2}}$$

the mixing coefficients depending on the asymmetry parameter. When  $\eta \rightarrow 0$ , then  $c_{-\frac{1}{2},\frac{3}{2}}$  and  $c_{-\frac{1}{2},\frac{1}{2}} \rightarrow 0$ . Only one frequency is observed [Figure 5(a)]

$$\nu_Q = \frac{1}{2}(e^2qQ/h)\left(1 + \frac{\eta^2}{3}\right)^{\frac{1}{2}} \quad (16)$$

and the values of  $e^2qQ/h$  and  $\eta$  cannot be separately deduced from experiments in zero magnetic field. For higher half-integral spins, there are  $(I + \frac{1}{2})$  such pairs, e.g.  $I = \frac{5}{2}$  nuclei (<sup>17</sup>O, <sup>27</sup>Al, <sup>127</sup>I) give three sets of Kramers doublets [Figure 5(b)] and in the general case of  $\eta \neq 0$ , three transitions can be observed  $\pm\frac{1}{2} \rightarrow \pm\frac{3}{2}(\nu_1)$ ,  $\pm\frac{3}{2} \rightarrow \pm\frac{5}{2}(\nu_2)$ , and  $\pm\frac{1}{2} \rightarrow \pm\frac{5}{2}(\nu_3)$ , where  $\nu_3 = \nu_1 + \nu_2$ , from whose values the quadrupole coupling constant and asymmetry parameter can be directly calculated by substitution into equations derived from a solution of the quadrupole Hamiltonian.<sup>27</sup> Similar comments apply to higher half-integral spins such as  $\frac{7}{2}$  (<sup>59</sup>Co) and  $\frac{9}{2}$  (<sup>209</sup>Bi). The levels are customarily labelled by the appropriate value of the nuclear magnetic quantum number  $m_1$ , a terminology which unfortunately is inexact: equation 15 shows that considerable mixing of the  $m_1$  substates occurs, and higher-order transitions such as  $\pm\frac{1}{2} \rightarrow \pm\frac{5}{2}$  for spin  $\frac{5}{2}$  become allowed when  $\eta \neq 0$ . All solutions for half-integral spins have one useful property: if  $\eta = 0$ , the transition frequencies between adjacent levels form an harmonic set, that is in Figure 5(b)  $\nu_2 = 2\nu_1$ , enabling this case to be easily identified, i.e. for <sup>59</sup>Co quadrupole resonance in  $[\text{Co}(\text{C}_5\text{H}_5)_2]^+ \text{ClO}_4^-$ , the observed frequencies are close to 12, 24, and 36 MHz.<sup>28</sup>

<sup>26</sup> A. Abragam and B. Bleaney, 'Electron Paramagnetic Resonance of Transition Ions', Clarendon Press, Oxford, 1970, p. 647.

<sup>27</sup> R. B. Creel, H. R. Brooker, and R. G. Barnes, *J. Magn. Reson.*, 1980, **41**, 146.

<sup>28</sup> J. Voitländer, H. Klocke, R. Longino, and H. Thieme, *Naturwissenschaften*, 1962, **49**, 491.

The nuclear quadrupole resonance frequencies we have just been discussing can be detected with the same kind of spectrometer as is used for nuclear magnetic

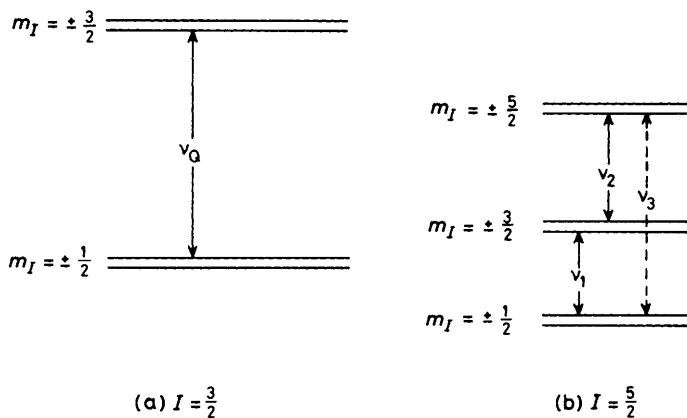


Figure 5 Energy level diagram for (a) spin  $\frac{3}{2}$  ( $^{11}\text{B}$ ,  $^{35}\text{Cl}$ ) and (b) spin  $\frac{5}{2}$  ( $^{17}\text{O}$ ,  $^{127}\text{I}$ )

resonance studies of solids, whether c.w. (continuous wave) or pulsed; the magnet is simply removed and the spectrometer tuned to the resonance frequency to be detected. Therein lies the chief difficulty; most magnetic resonance spectrometers (with the exception of the new 'multi-nuclear' kind) operate at one or more fixed frequencies according to the gyromagnetic ratio of the nucleus under study and the value of the steady magnetic field; in nuclear quadrupole resonance spectroscopy however the frequency must be swept over a wide range, perhaps several octaves, in searching for quadrupole transitions, and the sensitivity and operating conditions must be kept constant during this search. These requirements account for the popularity of frequency-swept oscillators, whether limited<sup>29</sup> or super-regenerative<sup>30</sup> in kind, in which the frequency can be changed by slowly varying the tuning capacitor in the tank circuit of the oscillator, of which the r.f. coil surrounding the sample forms the other component. Variable-frequency oscillators of this kind have formed the basis of several commercial spectrometers.<sup>31,32</sup> It should be borne in mind that no single r.f. coil will cover the whole range of quadrupole resonance frequencies, although the same basic design of oscillator can be used to span the frequency range from 5 to 700 MHz, with simple modifications such as the use at higher frequencies of a 'butterfly' capacitor as the frequency controlling element.<sup>33</sup> As with other solid state measurements, the lines are broad, often 1 kHz or more wide, and the sensitivity is not high, but since the range of observed frequencies is large, the 'effective resolution' can be high. Variable-frequency pulsed spectro-

<sup>29</sup> F. N. H. Robinson, *J. Phys. E*, 1982, **15**, 1093.

<sup>30</sup> H. C. Torrey, *Phys. Rev.*, 1949, **75**, 1326; D. Williams, *Physica*, 1951, **17**, 454.

<sup>31</sup> J. A. S. Smith and D. A. Tong, *J. Sci. Instrum.*, 1968, **1** (ser. 2), 8.

<sup>32</sup> J. A. S. Smith, *J. Chem. Educ.*, 1971, **48**, 39, A77, A147, A243.

<sup>33</sup> P. Butcher, J. A. S. Smith, and C. J. Turner, *J. Phys. E*, 1979, **12**, 484.

meters afford the possibility of measuring the relaxation times  $T_1$  and  $T_2$  by methods essentially identical in principle to those used in nuclear magnetic resonance,<sup>25</sup> although large r.f. peak powers are needed. Of course, one may be studying multi-level (and non-equispaced) spin systems in quadrupole resonance spectroscopy, so that  $T_1$  relaxation decays are not necessarily exponential. They are for spin- $\frac{3}{2}$  systems, which have only a pair of levels;<sup>34</sup> with a three-level system, however, such as a spin-1 nucleus like  $^{14}\text{N}$ , there are three relaxation transition probabilities which may be labelled  $W_x$ ,  $W_y$ ,  $W_z$  (Figure 4) and the measured  $T_1$  may be governed by some combination of these which depends on the kind of relaxation experiment performed;<sup>35</sup> in an experiment, for example, in which the sample is subject to a string of '129°' pulses, and the 'steady-state' signal  $S(t)$  which builds up after each pulse studied as a function of the pulse interval  $t$ , then

$$\frac{(\infty) - S(t)}{S(t)} = e^{-t/T_{1(x)}} \quad (17)$$

where

$$T_{1(x)}^{-1} = 2 \left\{ W_x + \left( \frac{1}{W_y} + \frac{1}{W_z} \right)^{-1} \right\} \quad (18)$$

In principle, a study of all three relaxation times for the three observed transitions will give separate values for the three relaxation transition probabilities. Pulsed Fourier-transform techniques may also be used, although with typical r.f. powers available it is usually only possible to cover a narrow range of the spectrum at one r.f. carrier frequency.

A number of cases is known in which quadrupole resonance lines show fine structure, one of the most interesting being  $^{14}\text{N}$  quadrupole resonance in solid nitrogen;<sup>36</sup> the spectrum shown in Figure 6 was recorded on a frequency-swept Robinson oscillator<sup>29</sup> with frequency modulation and phase-sensitive detection. In this mode, the output is the slope, or first derivative, of the absorption curve. With an annealed sample and cancellation of the earth's magnetic field, the  $^{14}\text{N}$  lines are sufficiently sharp (about 0.7 kHz in width) to reveal a fine structure, assigned to a dipole-dipole coupling between the two N nuclei; the sign of this interaction is known from the known gyromagnetic ratio and adding it to the quadrupolar Hamiltonian, equation 12, as a small perturbation, and solving the resulting equation by the method of first-order perturbation theory gives a frequency spectrum the order of intensities of which depends on the sign of the  $^{14}\text{N}$  quadrupole interaction. For the result shown in Figure 6, the sign must be negative. Now  $Q$  for  $^{14}\text{N}$  is positive and a recent study<sup>37</sup> of the hyperfine structure in the  $2p3p^1P_1$  excited state of  $\text{N}^+$  (the electronic ground state of N has S symmetry and generates no electric field gradient at the nucleus) gives a value of  $+1.93(8) \text{ fm}^2$ . Thus  $q$  is negative in the  $\text{N}_2$  molecule in the solid, in agreement with the results of

<sup>34</sup> M. J. Weber, *J. Phys. Chem. Solids*, 1961, **17**, 267.

<sup>35</sup> S. Vega, *J. Chem. Phys.*, 1974, **61**, 1093; G. Petersen and P. J. Bray, *J. Chem. Phys.*, 1976, **64**, 522.

<sup>36</sup> J. R. Brookeman, M. M. McEnnan, and T. A. Scott, *Phys. Rev. B*, 1971, **4**, 3661.

<sup>37</sup> H. Winter and H. J. Andrä, *Phys. Rev. A*, 1980, **21**, 581.

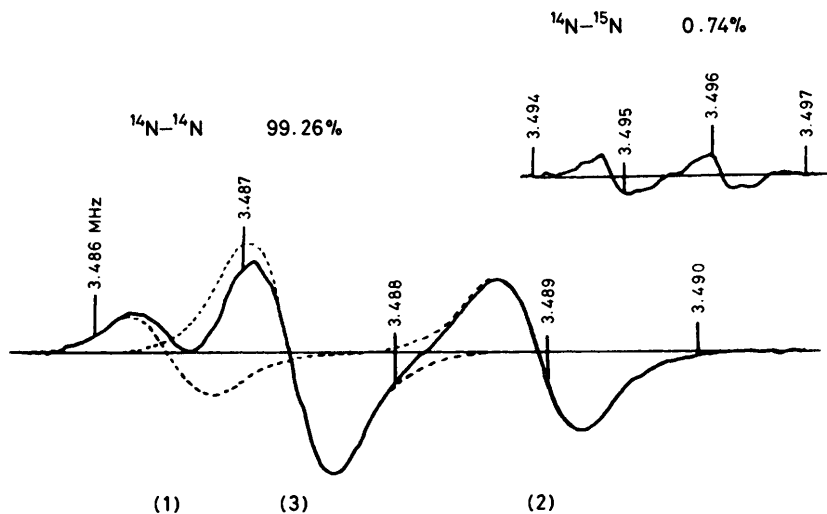


**Figure 6**  $^{14}\text{N}$  quadrupole resonance spectrum of  $\alpha\text{-N}_2$  at 4.2 K; the first derivative curve for  $^{14}\text{N}_2$  has been fitted to a superposition of three derivative curves of a 1:3:2 triplet (dotted lines) arising from the intra-molecular dipole-dipole coupling between the two  $^{14}\text{N}$  nuclei

a microwave determination<sup>38</sup> in  $^{15}\text{N}^{14}\text{N}$ , which gives a quadrupole coupling constant of  $-5.04$  MHz, slightly larger than the value of  $-4.65$  MHz found in the solid state and close to theoretical estimates.<sup>39</sup> Much of this difference can be accounted for by the moderating effect of large-amplitude torsional oscillations in the solid state, a factor which must be allowed for in all nuclear quadrupole resonance studies, and which make an important contribution to the commonly observed temperature-dependence of nuclear quadrupole resonance frequencies. An important feature of this investigation is the determination of the *sign* of the quadrupole coupling constant; such an inference is not usually possible in 'pure' nuclear quadrupole resonance unless the system is perturbed by some additional interaction of known sign, in this case a dipolar coupling.

Like most solid-state methods in nuclear magnetic resonance spectroscopy, the techniques so far described for nuclear quadrupole resonance require substantial samples, often 2 to 5 g, for investigations above 30 MHz, rising to 30 to 50 g at lower frequencies. However, there now exists a number of techniques capable of increasing the sensitivity of detection and so reducing the sample sizes required or the isotopic abundance needed to give detectable signals. One of these, that of double resonance, will be discussed in a following section. The remainder, to be discussed here, abandon altogether the idea of detecting the change in orientation of the nuclear quadrupole in an electric field gradient by means of the alternating e.m.f. induced in the sample coil. The first of these to be discussed (o.d.m.r., optically

<sup>38</sup> See reference 19, Chapter XIV.

<sup>39</sup> P. L. Cummins, G. B. Bacskay, and N. S. Hush, *J. Phys. Chem.*, 1985, **89**, 2151.

detected magnetic resonance) uses optical detection of the change,<sup>40</sup> and has the remarkable advantage of being able to measure quadrupole interactions in excited molecular states in solids. The principle of the method is shown in Figure 7; the molecule to be studied must have appropriate singlet ( $S_1$ ) and triplet ( $T_1$ ) excited

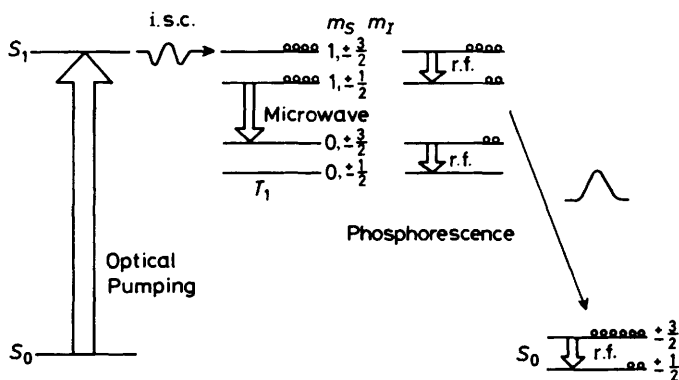


**Figure 7** A simplified transfer scheme for the optical detection of  $^{35}\text{Cl}$  quadrupole resonance in singlet ( $S_0$ ) and triplet ( $T_1$ ) states of *p*-dichlorobenzene

states, both split by the quadrupole interaction. Optical pumping to the excited singlet ( $S_1$ ) is followed by fast intersystem crossing (i.s.c.) to the triplet ( $T_1$ ) whose spin states, split because of dipolar coupling between the two electrons, are selectively populated owing to the symmetry-dominated intersystem selection rules. The triplet sub-levels then phosphoresce to the singlet ground state ( $S_0$ ), usually at different rates. Let us suppose that the state  $m_s = +1$  is selectively populated (Figure 7). Strong irradiation in the microwave region, corresponding to the transition  $\Delta m_s = -1$ ,  $\Delta m_l = \pm 1$ , partially allowed because of the electron-nucleus hyperfine interaction, transfers this order to the nuclear spins, preferentially populating the  $\pm \frac{3}{2}$  states and phosphorescence carries this polarization to  $S_0$  (provided that spin-lattice relaxation is slow enough). Repetition of the cycle builds up a strong 'pseudo-equilibrium' polarization, which leads to a decrease in the observed phosphorescence because of population depletion of the microwave-connected states. Irradiation at the  $^{35}\text{Cl}$  quadrupole resonance frequency in either  $S_0$  or  $T_1$  destroys this polarization and restores the original phosphorescence intensity; a plot of this intensity against radiofrequency (r.f.) therefore gives two groups of lines corresponding to  $^{35}\text{Cl}$  transitions in singlet ( $S_0$ ) and triplet ( $T_1$ ) states. In *p*-dichlorobenzene (Table 1), a difference in frequency of about 2.6 MHz is observed, together with an in-plane rotation of the direction of  $q_{zz}$  by  $12^\circ$  (from Zeeman measurements), attributed to a substantial distortion towards an anti-quinoid structure in the triplet state. Such methods are essentially double resonance experiments in which the quadrupole transitions are detected optically;

<sup>40</sup> K. P. Dinse and C. v. Borczyskowski, *Chem. Phys.*, 1979, 44, 93.

as such, they have high sensitivity, concentrations of  $10^{-5}$  molar being acceptable, but single crystals need to be used and low temperatures, usually 4.2 K, to prevent loss of information by fast quadrupole relaxation.

**Table 1**  $^{35}\text{Cl}$  quadrupole resonance frequencies  $\nu_Q(\text{MHz})$  in the singlet ground (S) and triplet excited (T) states of *p*-dichlorobenzene measured in various matrices at 1.2 K

Matrix	$\nu_Q(S)$	$\nu_Q(T)$
<i>p</i> -dichlorobenzene	34.831 *	32.25
Toluene	35.91	32.61
<i>p</i> -dibromobenzene	34.878	32.35

• At 4.2 K

The second group are often referred to as nuclear methods, because they detect quadrupole interactions by their influence on the angular distribution of  $\beta$  or  $\gamma$ -emissions from the nucleus under investigation, providing thereby a very high sensitivity of detection. The technique is by no means confined to naturally occurring radioactive nuclei. Almost all stable atomic nuclei in the Periodic Table can exist in excited states to which they may be promoted by particle bombardment or radioactive decay of a suitable precursor, and which subsequently decay by  $\beta$  or  $\gamma$ -emission. Now the probability of such emission depends on the angle between the nuclear spin axis and the direction in which the emission is being observed; in the case of  $\beta$ -emission, this anisotropy arises from parity non-conservation. Suppose the excited nuclear state whose emission is being studied is quadrupolar: simply cooling a single crystal of the sample to very low temperatures (a few mK) will magnetically polarize it by preferentially populating the lower energy levels, resulting in an anisotropy of the  $\beta$ -emission from which the quadrupole interaction and its sign can be deduced. The method is referred to as 'nuclear orientation', and is vastly improved in resolution by simultaneously irradiating at the suspected quadrupole resonance frequency which perturbs the populations and changes the  $\beta$ -anisotropy.<sup>41</sup>  $\beta$ -Emitting nuclei are particularly appropriate for this kind of experiment because they tend to have lifetimes long enough (1 to 100 ms) for r.f. irradiation to be effective. Polarized  $\beta$ -active excited nuclei can also be produced by bombardment with a beam of polarized neutrons, typical examples being  $^8\text{Li}(I = 3, t_{1/2} = 0.84 \text{ s})$ ,  $^{20}\text{F}(I = 2, t_{1/2} = 16 \text{ s})$ , and  $^{28}\text{Al}(I = 3, t_{1/2} = 3.2 \text{ min})$  produced by neutron capture by  $^7\text{Li}$ ,  $^{19}\text{F}$ , and  $^{27}\text{Al}$  respectively. Relative concentrations of about 1 part in  $10^{15}$  and polarizations of about 10% may be achieved.

Many more nuclei become eligible if  $\gamma$ -emitters are included. Their lifetimes, however, tend to be much shorter, typically  $10^{-5}$  to  $10^{-9}$  s, and the methods we have been discussing in previous paragraphs do not apply. Two main groups of techniques may then be used; those of time-differential perturbed angular correlations (PAC) or distributions (PAD). The principle of both is similar: consider an excited nuclear state, created for example by particle bombardment or radioactive decay. In PAC methods, the nucleus, after production or implantation

<sup>41</sup> H. Ackerman, D. Dubbers, and H. J. Stöckmann, *Adv. Nucl. Quad. Res.*, 1978, 3, 1.

in a suitable host, is required to decay to its ground state by the emission in rapid succession of two radiations, the intermediate state being quadrupolar: say both are  $\gamma$ -rays,  $\gamma_1$  and  $\gamma_2$ . Because of the dependence of radioactive emission on the angle between the nuclear spin axis and the direction of observation, the detection of  $\gamma_1$  in a fixed direction in a polycrystalline sample picks out only these nuclei whose spins lie in a preferred orientation, so the subsequent  $\gamma_2$  emission will show a definite angular correlation with the first. In PAD methods, which are in principle more general, the excited nuclear state should be quadrupolar and the alignment is produced by the nuclear reaction with the beam, substrates with small  $|m_1|$  being preferentially populated. Experimentally, in both cases one locates two counters at a fixed angle to each other (say  $90^\circ$ ) and to the incident beam and records the number of coincidences. The excited nuclear states can be generated in a number of ways. In PAD experiments on  $^{19}\text{F}$ , for example, bombardment with pulsed 0.5 MeV protons generated in a particle accelerator can provide sufficient  $^{19}\text{F}^*$  nuclei of spin  $\frac{5}{2}$ , quadrupole moment about  $7 \text{ fm}^2$ , and lifetime 128 ns. Each counter records a signal which decays exponentially with a lifetime of 128 ns, on which is superimposed an oscillatory perturbation generated by the change in angle between the nuclear spin axis and the direction of observation caused by the quadrupole precession. Taking the difference in count rate at two angles  $90^\circ$  to each other gives the differential counting rate  $R(t)$

$$R(t) = 2 \left\{ \frac{N(180^\circ, t) - N(90^\circ, t)}{N(180^\circ, t) + 2N(90^\circ, t)} \right\} \quad (19)$$

and for the case of spin  $\frac{5}{2}$  in an axially-symmetric electric field gradient this quantity is directly related to the interaction factor  $G_2(t)$

$$G_2(t) = \sum_n S_{2n} \cos(n\omega_0 t) \quad (20)$$

where the amplitudes  $S_{2n}$  depend on the nuclear spin,  $n$  is an integer and

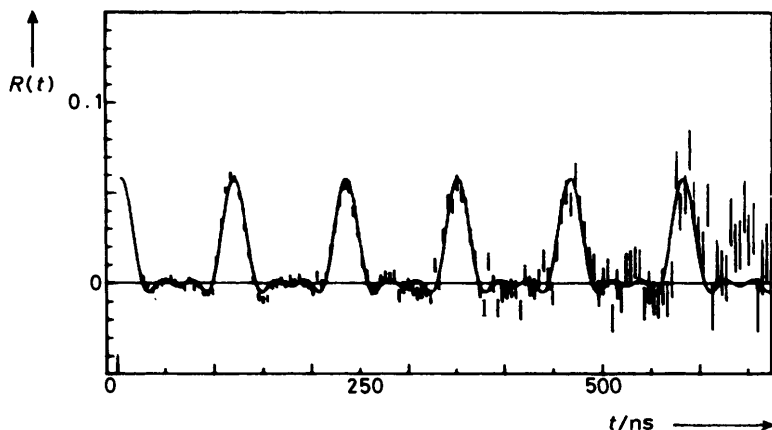
$$\omega_0 = 2\pi \left(\frac{3}{20}\right) (e^2 q Q / h)$$

Figure 8 shows a plot of  $R(t)$  for  $^{19}\text{F}^*$  PAC in  $\text{CF}_4$  at 15.5 K; the simply periodic pattern observed is typical of an asymmetry parameter of zero (or unity) in which  $R(t)$  is governed by  $G_2(t)$  in equation 20. Fourier transformation of the time-domain data gives a frequency spectrum  $P(\omega)$  containing the three harmonically related frequencies  $\nu_1, \nu_2, \nu_3$  for spin  $\frac{5}{2}$  when  $\eta = 0$ . The  $^{19}\text{F}$  quadrupole coupling constant is derived as 59.73 MHz ( $\eta = 0$ ).<sup>42</sup> The carbon tetrahalide series (apart from astatine) is now complete and the quadrupole coupling constants and asymmetry parameters are compared with those of the di-halogens in Table 2.<sup>43</sup> The significance of these results will be discussed in a later section.

<sup>42</sup> H. Barfuss, G. Bohnlein, C. Gradl, H. Hohenstein, W. Kreisliche, N. Niedrig, and A. Reimer, *J. Chem. Phys.*, 1982, **76**, 5103.

<sup>43</sup> G. K. Semin, T. A. Babushkina, and G. G. Jacobson, 'Nuclear Quadrupole Resonance in Chemistry', Leningrad, 1972, Appendix IV.





**Figure 8** Reduced counting rate  $R(t)$  for  $^{19}\text{F}$   $\gamma$ -ray emission in solid  $\text{CF}_4$  at 15.5 K as a function of the decay time

**Table 2** Halogen quadrupole coupling constants (MHz) in the diatomic halogen molecules and carbon tetrahalides

Nucleus	$e^2qQ/h$		$e^2qQ/h(\eta)$		
	MHz	T/K	MHz	T/K	
$^{19}\text{F}$	$\text{CF}_4$	59.73	15.5	$\text{F}_2$ 127.2 (0)	15.5
$^{35}\text{Cl}$	$\text{CCl}_4$	81 <sup>a</sup>	20	$\text{Cl}_2$ 107.74 (0.205) <sup>b</sup>	77
$^{79}\text{Br}$	$\text{CBr}_4$	640 <sup>a</sup>	77	$\text{Br}_2$ 759.83 (0.200) <sup>b</sup>	77
$^{127}\text{I}$	$\text{CI}_4$	2 130.33	77	$\text{I}_2$ 2 157.18 (0.175) <sup>b</sup>	77

<sup>a</sup> Average value. <sup>b</sup> See S. Sengupta, G. Litzistorf, and E. A. C. Lucken, *J. Magn. Reson.*, 1980, **41**, 169.

PAC(D) methods are sensitive, needing as few as  $10^8$  atoms, can be applied to powders, and in principle to all nuclei with  $Z > 18$ , plus F, Ne, and Na, but are not in general sign-determining. There are, however, problems particularly in molecular crystals. The resolution is limited by the lifetime of the isomeric level,  $\tau$ , through the well known expression

$$\Delta E \cdot \tau \geq h/2\pi \quad (21)$$

implying that  $\tau$  should not be shorter than 1 ns. Radiation damage may broaden the lines still further. Even more serious are the problems caused by the large recoil energy of the excited nucleus; in  $\text{CF}_4$ , 50% of the  $^{19}\text{F}^*$  atoms recoil back to the parent compound, which gives rise to a simple periodic time spectrum, but in  $\text{CHF}_3$ , the pattern is much more complex and needs to be explained in terms of two couplings, one of 58.72 MHz assigned to  $\text{C}-^{19}\text{F}$  and the other of 41.73 MHz assigned to  $\text{H}-^{19}\text{F}$  the latter having by far the larger amplitude.<sup>42</sup> Irradiation here has destroyed the parent molecule, creating a C-F-containing fragment and H-F, whose quadrupole interaction can thus be measured, although this was not presumably the original intention of the experiment. Clearly such effects will be

minimal in metals and alloys, to which field much present experimental activity is devoted.<sup>44</sup> In these materials, the probe nucleus may be selected and inserted into the host lattice by separation in a mass separator followed by ion implantation, the necessary high-energy ion beams, of 500 keV or more, being generated in special heavy-ion accelerators. Considerable radiation damage is often produced and may have to be reduced by annealing. At lower energies, suitable nuclei can be 'planted' on surfaces, and the high sensitivity of PAC measurements then makes it possible to measure the quadrupole (and magnetic) interactions of isolated atoms. Thus  $^{111}\text{Cd}$  ( $I = \frac{5}{2}$ ) may be planted on the 110 face of Al to a density of about  $10^9 \text{ cm}^{-2}$ ; 50% lie at terraced sites, with a quadrupole coupling constant of 176 MHz and asymmetry parameter of 0.1, the remainder apparently being distributed at kinks and defects on or near the surface.<sup>45</sup> The implication of these techniques for the study of catalysis is clear.

Another technique in which nuclear quadrupole interactions are detected by their effect on the  $\gamma$ -emission of excited nuclear states is that of Mössbauer spectroscopy, in which the excited nuclear state is created *in situ* by  $\gamma$ -radiation from the parent nucleus, and recoil problems are absent provided that the  $\gamma$ -ray energy  $E_\gamma < 150 \text{ keV}$ , when the lattice phonons are able to take up the recoil energy. The technique has been well discussed in several excellent textbooks,<sup>46</sup> and will be only briefly referred to here. The spectra are measured by moving the source of the  $\gamma$ -rays relative to the absorber, and splittings  $\delta\nu$  are usually quoted in velocity units,  $\delta\nu$ . To convert from these to Hz, one uses the relation  $\delta\nu = 2.418 \times 10^{14} E_\gamma \nu/c$ , in which  $E_\gamma$  is the  $\gamma$ -ray energy in eV. The lifetime of the excited nuclear state is short, often  $\leq 10^{-7} \text{ s}$ , so although the resolving power as a fraction of the  $\gamma$ -ray energy is remarkably large, about 1 in  $10^{37}$ , the lines tend to be broad, and from equation 21 quadrupole splittings smaller than  $(2\pi\tau)^{-1}$  cannot be resolved. Furthermore, only a relatively small number of nuclei can be studied, in practice about 25, because of the need to have a low-energy ground-state transition. However, signs can be measured in a number of cases; firstly, for spin states higher than  $\frac{3}{2}$ , from the unequal spacing of the lines; secondly for the  $\frac{3}{2} \longrightarrow \frac{1}{2}$   $\gamma$ -transition (and small asymmetry parameters) by application of a large magnetic field (e.g. 5 T or more) to a polycrystalline sample and a study of the observed splittings; thirdly, for single crystals showing quadrupolar splitting, by measurement of the line intensities as a function of the angle between the  $\gamma$ -ray direction and that of  $q_{zz}$ .<sup>46</sup>

#### 4 $^2\text{H}$ and $^{14}\text{N}$ Quadrupole Interactions in Solids

These two nuclei are grouped together because they both have spin-1 and have been extensively studied by the techniques of radiofrequency spectroscopy; however, their quadrupole coupling constants depend on electronic structure and molecular geometry in very different ways.

<sup>44</sup> H. Barfuss, G. Böhnlein, F. Gubitz, W. Kreische, and B. Röseler, *Hyperfine Interactions*, 1983, **15/16**, 815.

<sup>45</sup> H. Haas, *Z. Naturforsch. A*, 1986, **41**, to be published.

<sup>46</sup> T. C. Gibb and N. Greenwood, 'Mössbauer Spectroscopy', Chapman and Hall, London, 1971; A. Abragam, 'L'Effet Mössbauer', Gordon and Breach, New York and London, 1964.

$^2\text{H}$  has a very low nuclear quadrupole moment (the best present value being + 0.286 fm<sup>2</sup>) and quadrupole coupling constants are small, between 30 and 300 kHz. This rules out the use of the variable-frequency oscillator type of spectrometer; for many years, measurements have been performed by studying the quadrupole splitting of the  $^2\text{H}$  magnetic resonance spectra of single crystals,<sup>47</sup> a method to which we have not hitherto referred. The technique requires single crystals of about 1 cm<sup>3</sup> in volume, highly enriched in  $^2\text{H}$ . The sample is placed in a high magnetic field, high enough to ensure that the quadrupole splittings are only a small fraction (say one percent) of the  $^2\text{H}$  Zeeman frequency; under these conditions, the quadrupole splitting of the  $^2\text{H}$  magnetic resonance lines can be predicted by the use of first-order perturbation theory. Application of the magnetic dipole selection rule  $\Delta m_l = \pm 1$  then gives rise to *two* frequencies for each magnetically distinct  $^2\text{H}$  in the crystal, corresponding to the transitions  $-1 \rightarrow 0$  and  $0 \rightarrow +1$ , whose splitting  $\Delta\nu$  is orientation dependent; for example, if the crystal is rotated about the  $Z$ -axis,

$$\Delta\nu_z = A_z + B_z \cos 2\theta_x + C_z \sin 2\theta_x \quad (22)$$

in which  $\theta_x$  is the angle between the  $X$ -direction and the magnetic field and  $A_x =$

$$\frac{3}{4} \left( \frac{e^2 Q}{h} \right) (q_{xx} + q_{yy}), \quad B_z = \frac{3}{4} \left( \frac{e^2 Q}{h} \right) (q_{xx} - q_{yy}), \quad \text{and} \quad C_z =$$

$$\frac{3}{2} \left( \frac{e^2 Q}{h} \right) q_{xy}, \quad \text{where } q_{xx}, q_{xy}, \text{ etc. are the quadrupole coupling components in}$$

the crystal frame of reference. Rotating the crystal changes  $\theta_x$  and hence  $\Delta\nu_z$ ; the variation of  $\Delta\nu$  with  $\theta$  (the so-called 'rotation pattern') about a minimum of two different axes in the crystal is usually (not always) sufficient to give the *full* quadrupole tensor in the crystal axes, in which frame it is not necessarily diagonal and may therefore have to be transformed by standard procedures. Figure 9 shows such a pattern for LiOD.D<sub>2</sub>O at 82 K about the  $c$ -axis of this monoclinic crystal;<sup>48</sup> one pattern is almost invariant to rotation, and must correspond to an O-D<sup>-</sup> ion of low asymmetry parameter with its internuclear axis parallel to the rotation axis, the other two lines coming from the D<sub>2</sub>O molecules. Equation 22 then gives  $e^2 qQ/h = 271.7 \pm 1.0$  kHz,  $\eta = 0.043 \pm 0.005$  for O-D<sup>-</sup>;  $q_{zz}$  is parallel to  $c$  and  $q_{yy}$  to  $b$ .

The study of the quadrupole splitting of nuclear magnetic resonance lines is an important technique, especially if the crystal structure is known, since it then gives both the magnitude and orientation of the  $^2\text{H}$  principal components with respect to molecular-based axes; it has recently undergone a revival of interest with the increased availability of high-field solid-state cross-polarization spectrometers using superconducting magnets, which renders more nuclei eligible for studies of this kind, and of course increases sensitivity.<sup>49</sup> However, the use of single crystals is

<sup>47</sup> A. Weiss and N. Weiden, *Adv. Nucl. Quad. Res.*, 1980, 4, 149.

<sup>48</sup> J. O. Clifford, J. A. S. Smith, and F. P. Temme, *J. Chem. Soc., Faraday Trans. 2*, 1975, 71, 1352.

<sup>49</sup> S. Schramm and E. Oldfield, *J. Am. Chem. Soc.*, 1984, 106, 2502.

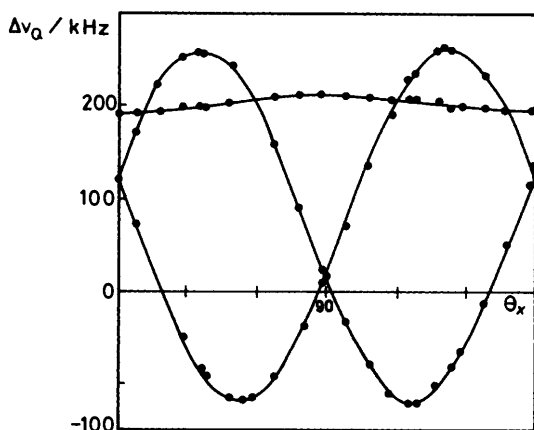


**Figure 9**  $^2\text{H}$  rotation pattern of  $\text{LiOD}\cdot\text{D}_2\text{O}$  about the  $c$ -axis of the monoclinic unit cell at 82 K

a serious disadvantage, particularly in the study of intractable materials such as deuterated polymers; fortunately a first-order splitting pattern obtained by taking a polycrystalline average of equation 22 can still be observed in powder samples. The pattern shows peaks or shoulders (Figure 10) from which values of the quadrupole coupling constant and asymmetry parameter can be deduced (but *not* the orientation). The  $^2\text{H}$  spectrum in Figure 10 of a drawn sample of deuterated polyethylene at 143 K shows differing contributions from the crystalline and amorphous regions as the angle  $\beta_0$  between the direction of order and the magnetic field is varied.<sup>50</sup> At low values of  $\beta_0$ , the spectrum of the crystalline region predominates, whereas both amorphous and crystalline regions contribute at values close to  $90^\circ$ . At higher temperatures the spectrum undergoes a marked narrowing as the  $-\text{CD}_2$  group begins to rotate. This experiment provides an important example of the sensitivity of quadrupole coupling constants to both structure and molecular motion; a study of relaxation times and frequencies and the variation of both with temperature gives information not only on the dynamics but also the mechanism, a theme to which we will return in the next section.

Another way of overcoming the difficulties in obtaining single crystals of sufficient size is to work in zero field, but overcome sensitivity problems by fast field cycling.<sup>51</sup>  $^2\text{H}$  magnetic resonance of a highly enriched polycrystalline sample is observed by means of a  $90^\circ$  pulse in the high magnetic field of a superconducting system (necessary to obtain good signal-to-noise ratio) and then the field is switched in two steps, one adiabatic the other sudden, to zero field in a very short time, where the nuclear quadrupole moments are allowed to process freely for a

<sup>50</sup> H. W. Spiess, *J. Mol. Struct.*, 1983, 111, 119.

<sup>51</sup> A. Bielecki, J. B. Murdoch, D. P. Weitekamp, D. B. Zax, K. W. Zilm, H. Zimmerman, and A. Pines, *J. Chem. Phys.*, 1984, 80, 2232.

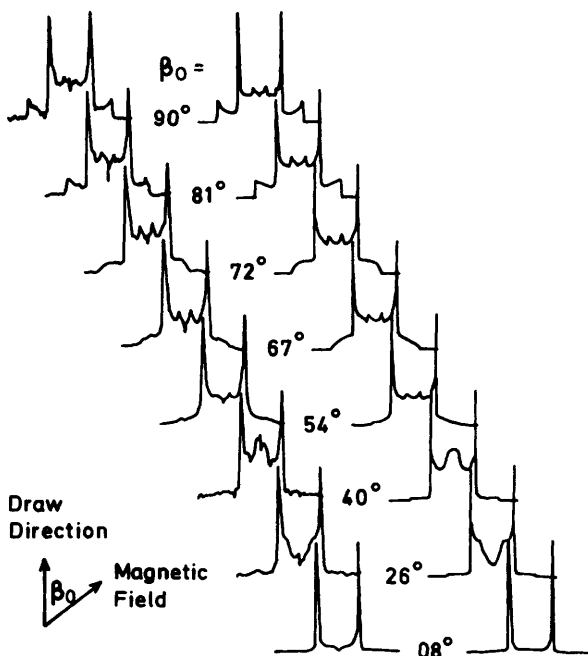


**Figure 10**  $^2\text{H}$  powder pattern at 143 K of a drawn sample of deuterated polyethylene at various angles  $\beta_0$  between the direction of order and the magnetic field. The observed spectra are given on the left and the calculated on the right

short time  $t$  (between say 3 and 1000  $\mu\text{s}$ ). The sample is now as rapidly returned to high field, where the time evolution of the quadrupole precession in zero field is monitored by a second  $90^\circ$  pulse to record the changed  $^2\text{H}$  magnetization. The process is repeated for different values of  $t$ ; a Fourier transform of the time-domain data then gives the  $^2\text{H}$  frequency spectrum. Figure 11 shows the  $^2\text{H}$  quadrupole resonance spectrum of polycrystalline perdeuterated 1,4-dimethoxybenzene obtained in this way; as a spin-1 nucleus, each chemically distinct  $^2\text{H}$  should show three lines  $\nu_x, \nu_y, \nu_z$ , (Figure 4) which for the aromatic nuclei in this spectrum are labelled  $A_0, A_1, A_2$  (for which  $e^2qQ/h = 178.5$  kHz,  $\eta = 0.045$ ) and  $B_0, B_1, B_2$  (for which  $e^2qQ/h = 179.1$  kHz,  $\eta = 0.067$ ). Note particularly the sharpness of the lines, and the ability of the technique to separate  $^2\text{H}$  signals of very similar quadrupole coupling constants and asymmetry parameters. But the sample still needs some degree of enrichment; this disadvantage is removed, at the cost of some loss of resolution, by double resonance techniques.

The principle of these methods is similar in some respects to that of  $^{13}\text{C}$  cross-polarization magnetic resonance. The resonance of the nucleus under study is detected (or enhanced) by coupling it to a spin- $\frac{1}{2}$  nucleus present (such as  $^1\text{H}$ ) with

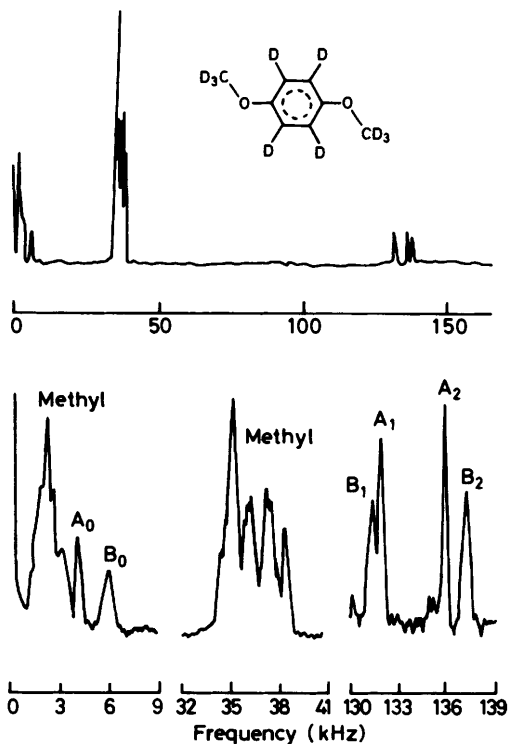


**Figure 11** Fourier transform  $^2\text{H}$  quadrupole resonance spectrum of perdeuterated-1,4-dimethoxybenzene at room temperature; the lower plots are expanded versions of the three spectral regions in the upper plot, corresponding (in order of increasing frequency) to the three groups of transitions  $\nu_z$ ,  $\nu_y$ , and  $\nu_x$ . Groups A and B are the aromatic deuteron signals

a much stronger magnetic resonance signal. The conflicting needs of high field to obtain a good  $^1\text{H(P)}$  signal, and zero field to excite the quadrupole (Q) resonance in a polycrystalline sample without Zeeman broadening, are resolved, as in the previous paragraph, either by fast field cycling or fast sample transfer. The sensitivity of such methods is high, sufficient in some cases to detect  $^2\text{H}$  signals in natural abundance,<sup>52</sup> if the whole sample transfer cycle, 'in' and 'out', is conducted under adiabatic conditions, in a time much shorter than the P and Q spin-lattice relaxation times. In adiabatic processes, in this case of adiabatic demagnetization, the entropy of the spin system is conserved; now a collection of spin- $\frac{1}{2}$  nuclei of splitting  $\Delta E = h\nu = \gamma H\hbar$  obeying Curie's equation has a molar entropy in a field  $H$  of

$$S = \frac{CH^2}{2T_s^2} \quad (23)$$

<sup>52</sup> D. T. Edmonds, *Phys. Rep.*, 1977, 29C, 233.

where  $C$  is Curie's constant and  $T_s$  is the spin temperature, defined by the Boltzmann distribution of populations between the two levels

$$\frac{n_{\text{upper}}}{n_{\text{lower}}} = e^{-\Delta E/kT} = e^{-\hbar\gamma H/kT}, \quad (24)$$

At the start of the double resonance experiment, the field is  $H_0$ , the field of the magnet, say 1 T. It might be thought that after switching off the magnet the field would be zero, but this neglects the small internuclear field always produced within a sample containing magnetic nuclei; we call this quantity  $H_L$ , the local field—it is capable of a precise definition<sup>53</sup> and in many proton-containing solids is of the order of a few tenths of a mT. Conservation of entropy means that during the first part of the field cycle

$$\left(\frac{H_0}{H_L}\right)^2 = \left(\frac{T_{\text{initial}}}{T_{\text{final}}}\right)^2 \approx (10^4)^2 \quad (25)$$

so that if the spin system was initially at room temperature, it is cooled by the reduction in field to a few tenths of a Kelvin. We now suppose that the quadrupolar levels are largely unaffected by the change in field—which is not true, but will not affect the present arguments. Hence, while adiabatic demagnetization 'cools' the  $^1\text{H}$  spins, it changes the Q spin temperature by very little. However, during the first part of the field cycle 'level-crossing' must occur (Figure 12) as the rapidly varying  $^1\text{H}$  levels collapse to zero, whilst the Q spins retain a non-zero splitting. At this level coincidence when the quadrupole (angular) frequency  $\omega_Q$  equals the  $^1\text{H}$  Larmor frequency  $\gamma_H H$ , the spin temperatures of the P and Q spin systems quickly equalize, so the Q spins (usually in low abundance) are strongly cooled and the P spins (usually in high abundance) are slightly warmed. In zero field, suppose we now irradiate with a strong r.f. field in the region in which one of the Q quadrupole resonance frequencies lies. If the irradiation frequency is 'off-resonance' nothing further occurs and on adiabatic remagnetization to high-field and further level-crossing, a slightly smaller  $^1\text{H}$  magnetization is monitored, which is independent of the zero-field irradiation frequency. If, however, we are 'on resonance', the Q levels may be saturated, *i.e.* heated to infinite spin temperature, and on return to high field a second level crossing warms up the  $^1\text{H}$  levels even more, and there is now a considerable reduction in their signal intensity observed in high field. A plot of  $^1\text{H}$  signal intensity in high field *versus* Q irradiation frequency in zero field, in a continuous cycle of this kind in which the Q frequency is stepped after each cycle, gives the zero field  $^2\text{H}$  quadrupole resonance spectrum.

The importance of measuring  $^2\text{H}$  quadrupole interactions lies in the rather unusual relationship they have to the electron distribution in the X–H bond; the 1s electron on the atom makes no contribution to the electric field gradient at the nucleus, which therefore depends through equation 7 on the inverse cube of the distance to the X nucleus and the electron distribution at this atom. Equation 7

<sup>53</sup> A. Abragam and W. Proctor, *Phys. Rev.*, 1958, **109**, 1441.

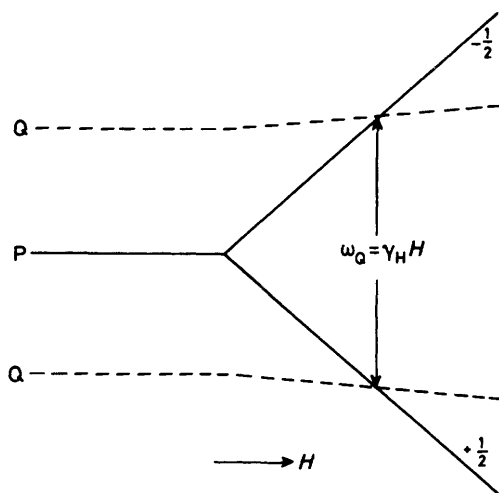


Figure 12 Diagrammatic representation of level-crossing for two-level P and Q spin systems

shows that these two terms are of opposite sign; the more concentrated positive charge of the X nucleus usually gains over the more diffuse electronic charge clouds, so  $q$  for  $^2\text{H}$  (as defined by equation 7) is usually positive and the quadrupole coupling constant likewise. For C–H bonds, the consequence is a significant dependence on the C–H distance;<sup>54</sup> a simple calculation will illustrate this: in atomic units, a charge of a  $1e$  at distance of 2 Bohr radii ( $1.11 \text{ \AA}$ ) will produce an electric field gradient,  $q$ , along the bond of  $+0.25$  from equation 4 and multiplying by  $2\ 349.6 Q$  gives  $+168 \text{ kHz}$ . Experimentally, quadrupole coupling constants for  $sp^3$ -hybridized bonds cluster around 160 to 170 kHz depending on the other substituents attached to the carbon atom, for  $sp^2$ -hybridized bonds around 180 kHz (*cf.* Figure 11), and for  $sp$ -hybridized bonds around 200 kHz, the order of decreasing C–H bond length. For O–H bonds, the consequence is a remarkable dependence on the strength of hydrogen bonding,<sup>55</sup> the  $^2\text{H}$  quadrupole coupling constant falling from  $+308 \text{ kHz}$  in HOD vapour to  $56 \text{ kHz}$  (sign unknown) in the symmetric O–H–O<sup>-</sup> hydrogen bond in potassium hydrogen maleate,<sup>56</sup> the drop following closely an inverse cube dependence on the O...H distance; at the same time the asymmetry parameter increases from 0.14 in the former to 0.52 in the latter. The low  $^2\text{H}$  quadrupole coupling constant and high asymmetry parameter furnish a particularly useful way of identifying and studying electronic structure in these short and symmetric (or near-symmetric) O–H–O hydrogen bonds.

For  $^{14}\text{N}$ , the same experimental methods that we have surveyed for  $^2\text{H}$

<sup>54</sup> P. L. Olympia Jr., I. Y. Wei, and B. M. Fung, *J. Chem. Phys.*, 1969, **51**, 1610.

<sup>55</sup> M. J. Hunt and A. L. MacKay, *J. Magn. Reson.*, 1974, **15**, 402; 1976, **22**, 295.

<sup>56</sup> T. Chiba, *J. Chem. Phys.*, 1964, **41**, 1352; I. J. F. Poplett, M. Sabir, and J. A. S. Smith, *J. Chem. Soc. Faraday Trans. 2*, 1981, **77**, 1651.



quadrupole resonance can be used, although its larger quadrupole interactions, between 50 and 5000 kHz, imply some changes in the experimental conditions. In general, the larger the quadrupole interactions, the more efficient is quadrupole relaxation and the shorter  $T_{1Q}$ , the quadrupole spin-lattice relaxation time, a factor which must be taken into account in devising the appropriate experiments.<sup>52</sup> There is one advantage:  $^{14}\text{N}$  resonance can very simply be detected in field cycling experiments in which no irradiation at the Q frequency need be applied. The  $^1\text{H}$  signal is, as usual, detected in high field which is then very rapidly changed to a small but finite value,  $H$ , such that the  $^1\text{H}$  frequency in this field matches one of the  $^{14}\text{N}$  quadrupole resonance frequencies

$$\omega_Q = \gamma_H H \quad (26)$$

In a short time, usually less than 1 ms, the two spin-systems come to a common spin temperature, just as in level-crossing; the difference now is that this matching condition continues to be maintained while the combined spin systems, P + Q, relax together with a relaxation time which is the weighted mean of the two relaxation times,  $T_1$  for the P spins and  $T_{1Q}$  for the Q, that is

$$\left\{ \left( \frac{\varepsilon}{1 + \varepsilon} \right) \frac{1}{T_{1Q}} + \left( \frac{1}{1 + \varepsilon} \right) \frac{1}{T_1} \right\}^{-1} \quad (27)$$

in which  $\varepsilon$  is  $2N_Q/3N_P$  and  $N_Q$  and  $N_P$  are the numbers of Q and P spins. Since  $T_{1Q}$  is usually much less than  $T_1$ , the proton magnetization drains away in a relatively short time, and on return to high field an immediate  $90^\circ$  pulse will reveal a much smaller recovered  $^1\text{H}$  signal, provided that the matching condition, equation 26, was satisfied in low field. The method, which has been called  $^{14}\text{N}$  quadrupole cross-relaxation spectroscopy,<sup>57</sup> is very successful in detecting  $^{14}\text{N}$  quadrupole resonance signals under normal experimental conditions, *i.e.* room temperature. All three signals  $v_x, v_y, v_z$  can be detected with similar sensitivity and the broadening and shift in frequency due to observation in a finite magnetic field is not serious unless the asymmetry parameter is close to zero. Figure 13 shows the complete  $^{14}\text{N}$  spectrum of 2-methylquinazolin-4-one, with the lines assigned to specific nitrogen atoms, giving at 291 K

$$\begin{array}{ll} > \text{N}-\text{CH}_3 & e^2qQ/h = 3.573 \text{ MHz}, \eta = 0.459 \\ -\text{N}= & e^2qQ/h = 5.530 \text{ MHz}, \eta = 0.061 \end{array}$$

Note the sharper unassigned lines at low frequencies; they occur at sub-harmonics of the fundamental  $^{14}\text{N}$  frequencies and are due to multi-proton relaxation jumps—as many as four have been observed to relax just one  $^{14}\text{N}$  nucleus in imidazole.

The values of  $^{14}\text{N}$  quadrupole parameters depend on the electron distribution around the atom, and since the  $s$ -electrons on the same atom contribute nothing, it is the contributions from the  $2p$  electrons which dominate. Strictly speaking, to provide a proper calculation of the electric field gradient from equation 7, the

<sup>57</sup> P. M. G. Bavin, D. Stephenson, and J. A. S. Smith, *Z. Naturforsch. A*, 1986, **41**, 195.

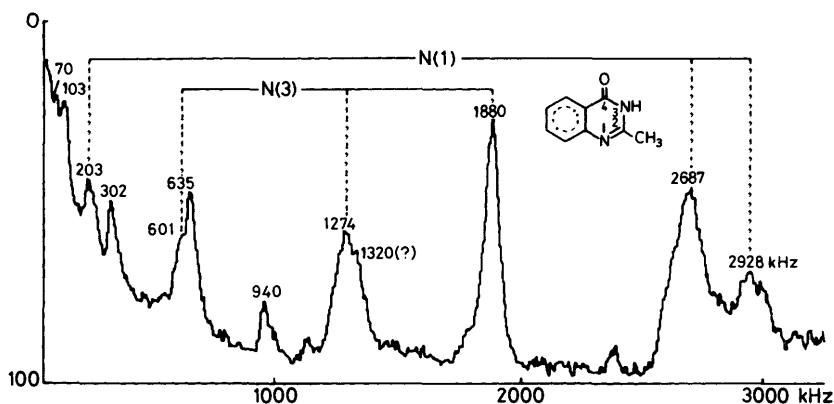


**Figure 13**  $^{14}\text{N}$  quadrupole cross-relation spectrum at 291 K of 2-methylquinazolin-4-one with line assignments indicated

molecular geometry must be accurately known and an electronic wave-function used of near Hartree–Fock SCF quality, with a basis set containing both core and valence shell atomic orbitals at least. Even then, it may be necessary to make some allowance for configuration interaction, and variations in geometry due to molecular vibrational modes.

Such calculations have been performed for diatomic molecules<sup>59</sup> such as  $\text{N}_2$ , and more complex molecules, *e.g.* five-membered heterocyclic systems such as 1,2,4-triazole and 1*H*-tetrazole,<sup>58</sup> with reasonable success. Frequently, however, one needs to make rough, rule-of-thumb calculations of the electronic significance of  $^{14}\text{N}$  quadrupole coupling constants, and for this purpose the theory of Townes and Dailey has found much application. Since the basic principles have been explained elsewhere,<sup>59</sup> we give here only a brief resumé. The effects of the nuclear charges and electronic charge clouds of neighbouring atoms are assumed to cancel each other; only the  $2p$  electron distribution of the nitrogen atom in question is considered, and variations in the Sternheimer factor from one molecule to another are neglected; and a value of  $e^2q_{zz}Q/h$  for one  $2p$  electron in a  $2p_z$  orbital at N is assumed to be known—a recent estimate is<sup>37</sup>  $-13.7$  MHz. Everything now depends on the distribution, or state of hybridization, of the  $2p$  electrons. If the directions of the principal axes are known, or can be inferred, a particularly simple situation arises; in gaseous  $\text{NH}_3$ , for example,  $q_{zz}$  lies along the threefold axis and equals  $-4.092(4)$  MHz, and  $\eta = 0$  (at least, in the gas, for these are microwave data<sup>60</sup>). The sign can be understood, since the lone-pair of electrons lies along the threefold axis and

<sup>58</sup> M. H. Palmer, D. Stephenson, and J. A. S. Smith, *Chem. Phys.*, 1985, **97**, 103.

<sup>59</sup> E. A. C. Lucken, 'Nuclear Quadrupole Coupling Constants', Academic Press, New York and London, 1969, Chapter 7.

<sup>60</sup> S. G. Kukolich and S. C. Wolfsy, *J. Chem. Phys.*, 1970, **52**, 5477.

dominates the quadrupole coupling constant;  $q$  is therefore negative,  $Q$  is known to be positive, so the quadrupole coupling constant is negative. To interpret the experimental value in more quantitative terms, we must assume a state of hybridization at the N atom; for example take  $sp^3$  hybrids for a regular tetrahedron

$$\varphi_1 = \frac{1}{2}\psi_s + \sqrt{\frac{3}{2}}\psi_z \quad (28)$$

$$\varphi_2 = \frac{1}{2}\psi_s + \sqrt{\frac{2}{3}}\psi_x - \frac{1}{2\sqrt{3}}\psi_z$$

$$\varphi_3 = \frac{1}{2}\psi_s + \frac{1}{\sqrt{2}}\psi_y - \frac{1}{\sqrt{6}}\psi_x - \frac{1}{2\sqrt{3}}\psi_z$$

$$\varphi_4 = \frac{1}{2}\psi_s - \frac{1}{\sqrt{2}}\psi_y - \frac{1}{\sqrt{6}}\psi_x - \frac{1}{2\sqrt{3}}\psi_z$$

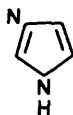
and an occupation number of 2 for  $\varphi_1$ , the lone pair of electrons, and  $b$  for the three N-H bonds  $\varphi_2, \varphi_3, \varphi_4$ . The actual HNH angle is less than tetrahedral, but this factor can be allowed for at the expense of greater complexity in equation 28. The actual system used in equation 28 for the  $2p_x(\psi_x)$ ,  $2p_y(\psi_y)$  and  $2p_z(\psi_z)$  orbitals is the same as that of the principal components; the contribution of each hybrid orbital to the  $^{14}\text{N}$  quadrupole coupling can therefore be evaluated from the first term on the right hand side of equation 7, setting  $\psi$  in turn equal to each of the four wave functions in equation 28. The lone pair orbital, for example, gives a contribution to  $q_{zz}$  of

$$-\frac{3}{2}e \int \psi_z^2 \left( \frac{3\cos^2\theta - 1}{r^3} \right) d\tau = \frac{3}{2} \left( \frac{e^2qQ}{h} \right)_0 \quad (29)$$

where  $(e^2qQ/h)_0$  is  $-13.7$  MHz. The contribution of the remaining three orbitals can be evaluated in a similar way, and the result is

$$(e^2qQ/h) = \frac{3}{2}(2 - b)(e^2qQ/h)_0 \quad (30)$$

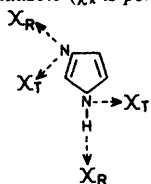
so the experimental value of  $-4.084$  MHz in the gas phase corresponds to  $b = 1.60$ . At the actual HNH angle of  $107.8^\circ$ , this value becomes  $1.57$ . In the solid, the quadrupole coupling constant drops to  $3.161$  MHz and  $b$  increases to  $1.67$ ; a major contribution to this change comes from polarization of the N-H bond caused by hydrogen bonding. The approximations inherent in this approach are obvious: the absolute values of the atomic populations have little significance, but



(1)

their differences often provide an extremely convenient way of interpreting quadrupole resonance data in terms of electronic structure in the solid state. Take a more complex system such as imidazole (1); simple considerations suggest that  $q_{zz}$  at N(3) lies in-plane roughly in the direction of the lone pair, and  $q_{zz}$  at NH lies perpendicular to the molecular plane, both being negative, as is inferred experimentally.<sup>61</sup> At 291 K, the values are given in Table 3 for the solid state, and compared with those obtained from microwave spectroscopy.<sup>62</sup> Now imidazole is hydrogen-bonded in the solid, the NH group of one molecule hydrogen-bonding to the  $-N=$  group of its neighbour, and this almost certainly accounts for much of the difference between the gas and solid-state values, as can be checked by calculation.<sup>63</sup> In contrast, the  $-N=$  group in 2-methylcinnolin-4-one, whose spectrum is given in Figure 13, has a much higher quadrupole coupling constant (5.530 MHz,  $\eta = 0.061$ ) since it is now 'free', the hydrogen bonding presumably occurring between the  $-NH-$  and CO group of neighbouring molecules.

**Table 3**  $^{14}\text{N}$  quadrupole coupling components ( $\chi$  in MHz) in gaseous (microwave) and solid (n.q.r.) imidazole ( $\chi_x$  is perpendicular to the molecular plane)



		$\chi_R$	$\chi_T$	$\chi_x$
N(1)H	Gas	1.494	1.403	-2.537
	Solid	0.049	1.342	1.391
N(3)	Gas	-4.032	1.774	2.258
	Solid	3.220	1.803	1.417

Co-ordination of N(3) in imidazole to a suitable metal ion has a similar but larger effect to that of hydrogen bonding,<sup>64</sup> with  $q_{zz}$  roughly in-plane along the direction of the lone pair and  $q_{xx}$  perpendicular to the plane (Table 3), a Townes–Dailey approach predicts that the quadrupole coupling constant will drop sharply in magnitude as electron donation from N(3) increases, and the asymmetry parameter will rise. So in  $\text{Cd}(\text{C}_3\text{N}_2\text{H}_4)_2\text{Cl}_2$   $e^2qQ/h = 2.35$  MHz,  $\eta = 0.36$ , corresponding to a donor orbital occupancy of 1.76, whereas in  $\text{Zn}(\text{C}_3\text{N}_2\text{H}_4)_2\text{Cl}_2$  (2.13 MHz,  $\eta = 0.57$ ) it falls to 1.72; the smaller Zn ion is more acidic than Cd and so withdraws more electrons from the co-ordinating N(3) atom.

## 5 $^{17}\text{O}$ Quadrupole Interactions

At first sight, the quadrupolar oxygen isotope,  $^{17}\text{O}$ , with a spin of  $\frac{5}{2}$  and an abundance of 0.037%, would seem to be an unlikely candidate for quadrupole resonance studies without some degree of enrichment. This can be done, at some expense, and recent  $^{17}\text{O}$  magnetic resonance studies<sup>65</sup> of a number of oxides have revealed first- and second-order quadrupolar splitting of the  $^{17}\text{O}$  magnetic

<sup>61</sup> M. L. S. Garcia, J. A. S. Smith, P. M. G. Bavin, and C. R. Ganellin, *J. Chem. Soc., Perkin Trans. 2*, 1983, 1391.

<sup>62</sup> G. Blackman, R. D. Brown, F. R. Burden, and I. R. Elsum, *J. Mol. Spectrosc.*, 1976, **60**, 63; D. Christen, J. H. Griffiths and J. Sheridan, *Z. Naturforsch. A*, 1982, **37**, 1378.

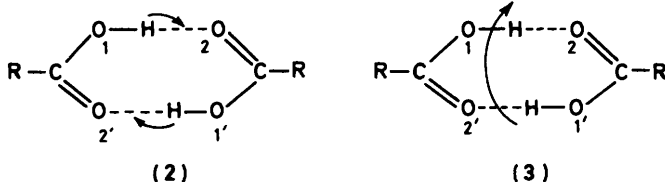
<sup>63</sup> M. H. Palmer, F. E. Scott, and J. A. S. Smith, *Chem. Phys.*, 1983, **74**, 9.

<sup>64</sup> C. I. H. Ashby, C. P. Cheng, and T. L. Brown, *J. Am. Chem. Soc.*, 1978, **100**, 6057.

<sup>65</sup> S. Schramm and E. Oldfield, *J. Am. Chem. Soc.*, 1984, **106**, 2502.

resonance lines from which approximate values for the  $^{17}\text{O}$  quadrupole coupling constants and asymmetry parameters have been deduced. Double resonance techniques are, however, sufficiently sensitive to detect  $^{17}\text{O}$  quadrupole resonance in natural abundance in many compounds whose  $^1\text{H}$  spin-lattice relaxation times in low magnetic field are sufficiently long—in practice, this means 1s or more. Signals from  $^{17}\text{O}-\text{H}$  or  $^{17}\text{O}\cdots\text{H}$  groups are of particular interest, since  $^{17}\text{O}\cdots\text{H}$  dipolar splitting can often be resolved, and from this the sign of the  $^{17}\text{O}$  quadrupole coupling constant and the rough orientation of the principal axes with respect to the  $\text{O}-\text{H}$  direction can be deduced.<sup>66</sup>

An interesting example of the usefulness of such studies occurs in the hydrogen-bonded carboxylic acid dimers (2), which are planar or nearly planar systems in which one of the principal components is obliged by symmetry to be perpendicular to the molecular plane. Now such dimers have been known for some years to suffer from proton disorder, and two possible mechanisms have been proposed to



account for this: fast concerted two-proton jumps across the hydrogen bond (2), or a rotation of the eight-membered ring of the dimer about the  $\text{C}\cdots\text{C}$  axis (3). Other physical methods have so far proved unable to distinguish between the two mechanisms, but the problem can be resolved in favour of mechanism (2) by  $^{17}\text{O}$  quadrupole double resonance studies.<sup>67</sup> Consider model (2); in the disordered crystal, the 'new'  $^{17}\text{O}$  principal quadrupole tensor of the  $\text{C}-^{17}\text{OH}$  group (or its centrosymmetrically related partner in the dimer) is simply derived by averaging the 'ordered'  $\text{C}-^{17}\text{OH}$  ( $\mathbf{D}_1$ ) and  $\text{C}=\text{O}\cdots\text{H}$  ( $\mathbf{D}_2$ ) tensors in a common frame of reference

$$\mathbf{D} = (1 - \alpha)\mathbf{D}_1 + \alpha\mathbf{D}_2 \quad (31)$$

where  $\alpha$  is the degree of mixing, and re-diagonalizing the new tensor  $\mathbf{D}$  to get the principal components in the disordered crystal. If  $\mathbf{D}_1$  and  $\mathbf{D}_2$  are known from previous studies of ordered crystals and change little with temperature or environment, then as  $\alpha$  increases, *i.e.* by an increase in temperature or by a suitable change of the substituent  $\text{R}$ , the  $\text{C}-^{17}\text{OH}$  and  $\text{C}=\text{O}\cdots\text{H}$  frequencies and quadrupole parameters will be observed to move together, finally becoming identical (or nearly so) at  $\alpha = 0.5$  when the two tensors (in the isolated molecule) become the same. This is not true in model (3), which simply rotates each tensor separately by  $180^\circ$ ; averaging again occurs, but as  $\alpha$  approaches 0.5, the  $\text{C}-^{17}\text{OH}$

<sup>66</sup> I. J. F. Poplett, *Adv. Nucl. Quad. Res.*, 1980, 4, 115.

<sup>67</sup> A. Gough, M. M. I. Haq, and J. A. S. Smith, *Chem. Phys. Lett.*, 1985, 117, 389.

and  $C=^{17}O \cdots H$  tensors still remain different, because one is not being transformed into the other. Figure 14 shows a plot of  $e^2qQ/h$  against  $\eta$  for the ring  $C-^{17}OH$  and  $C=^{17}O \cdots ^1H$  groups in nine different carboxylic acids known to form dimers in the solid state. The continuous curves give predictions for these quantities based on equation 31 and tensors  $D_1$  and  $D_2$  taken from results for ordered crystals containing  $-COOH$  groups; the values of  $\alpha$  are placed at appropriate intervals along the curve. The apparent 'reflections' near 7 MHz at the  $\eta = 0$  axis and 5.7 MHz at  $\eta = 1$  are simply due to interchanges in the directions of the principal components, and are a consequence of the Laplace equation and our use of the convention in equation 8: the first corresponds to an interchange in the directions of  $q_{xx}$  and  $q_{yy}$  which occurs whenever  $|q_{xx}|$  becomes larger than  $|q_{yy}|$ , and the second  $q_{yy}$  and  $q_{zz}$  which occurs when  $|q_{yy}|$  becomes larger than  $|q_{zz}|$ . It is seen that there is a good fit between theory and experiment, the  $C-^{17}OH$  and  $C=^{17}O \cdots H$  points almost coinciding for benzoic acid, which is known from other physical measurements to be almost completely disordered at room temperature. Note that the common drug aspirin (points 8 on Figure 14) is about 23% disordered at room temperature.

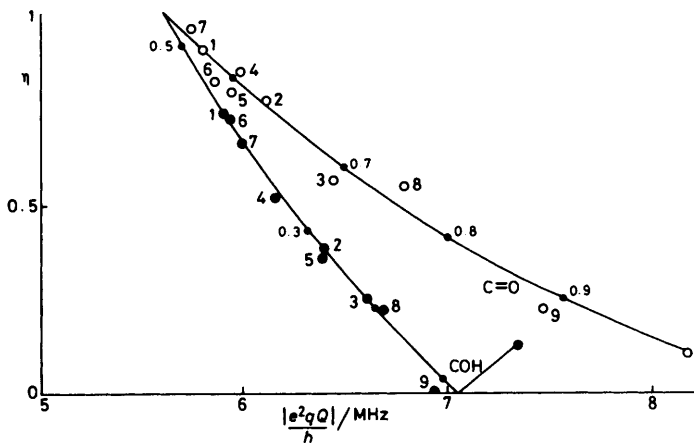


**Figure 14** A plot of  $^{17}O$  quadrupole coupling constants against asymmetry parameter for some carboxylic acid dimers at room temperature: open circles  $C=^{17}O \cdots H$  and closed circles  $C-^{17}OH$ . The experimental points refer to (1) benzoic acid, (2) *p*-chlorobenzoic acid, (3) *m*-chlorobenzoic acid, (4) *p*-nitrobenzoic acid, (5) *m*-nitrobenzoic acid, (6) *p*-hydroxybenzoic acid, (7) *m*-hydroxybenzoic acid, (8) acetylsalicylic acid, and (9)  $\beta$ -oxalic acid

This example illustrates the power of quadrupole resonance methods in clarifying modes of molecular motion; the same is true of the mechanism of phase transitions, *e.g.* in the alkali metal dihydrogen phosphates, in which  $^1H$  jumps also occur in a double potential well. In  $KH_2PO_4$ , all the protons move in a double potential well above 120 K, the Curie temperature ( $T_C$ ), and freeze into one of the two equilibrium sites below; the  $^{17}O$  quadrupole resonance frequencies of the

$P=^{17}\text{OH}$  and  $P=^{17}\text{O}\cdots\text{H}$  groups thus show<sup>68</sup> a similar behaviour to that predicted by equation 31, as is seen in Figure 15. Each pair of frequencies for the  $\pm\frac{1}{2}\rightarrow\pm\frac{3}{2}$ ,  $\pm\frac{3}{2}\rightarrow\pm\frac{5}{2}$ , and  $\pm\frac{1}{2}\rightarrow\pm\frac{5}{2}$  transitions of a spin- $\frac{5}{2}$  nucleus [Figure 5 (b)] collapses as the Curie temperature is approached from below, and equation 31 may still be used with  $\alpha$  redefined as the order parameter. Once again, the  $^{17}\text{O}$  quadrupole double resonance data provide a distinction of mechanism; they are inconsistent with a displacive model, in which the proton is off-centre below  $T_C$ , and moves to a central position above, because then the high temperature  $^{17}\text{O}$  tensor would *not* be the average of the two low-temperature ones.

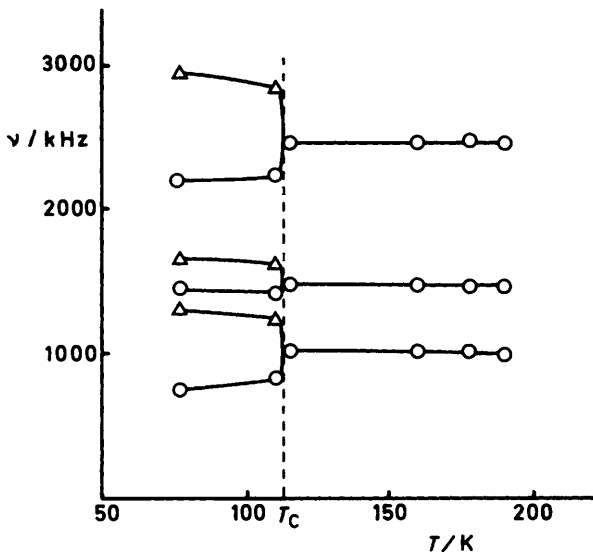


**Figure 15** Temperature variation of the  $^{17}\text{O}$  quadrupole double resonance frequencies in  $\text{KH}_2\text{PO}_4$ .

Nuclear quadrupole resonance and relaxation have been much used in recent years to study the mechanism and dynamics of phase transitions; the interested reader must be referred elsewhere for an authoritative review.<sup>69</sup>

## 6 Nuclear Quadrupole Interactions of Heavier Nuclei

In this concluding section, we look briefly at the quadrupole interactions of heavier nuclei than  $^{17}\text{O}$ , where all of the techniques referred to in previous sections may find application.

The halogens  $^{19}\text{F}^*$ ,  $^{35}\text{Cl}$ ,  $^{37}\text{Cl}$ ,  $^{79}\text{Br}$ ,  $^{81}\text{Br}$ ,  $^{127}\text{I}$ , and  $^{211}\text{At}$  are often singly bonded and for such a geometry the Townes–Dailey theory predicts a simple dependence

<sup>68</sup> R. Blinc, J. Seliger, R. Osredkar, and T. Prelesnik, *Chem. Phys. Lett.*, 1973, **23**, 486.

<sup>69</sup> H. M. Van Driel, M. Wiszmiewska, B. M. Moores, and R. L. Armstrong, *Phys. Rev. B*, 1972, **6**, 1596.

on the ionic character of the M–X bond ( $i$ ) and the degree of  $s$ -hybridization ( $s$ ) at the halogen, X;

$$\frac{(e^2qQ/h)_{MX}}{(e^2qQ/h)_0} = (1 - i)(1 - s) \quad (32)$$

where  $(e^2qQ/h)_0$  is the quadrupole coupling constant of one electron in a  $np_z$  orbital, often equated (but with opposite sign) to that observed in the halogen atom, e.g. 109.7 MHz in chlorine. Now the ionic character should depend on the electronegativity difference  $\chi_M - \chi_X$ ,  $\chi$  being the Pauling electronegativity; taking the results for the  $CX_4$  series in Table 2, and rather arbitrarily assuming  $s$  to be zero if the electronegativity difference is less than 0.25, 0.15 if it is greater, gives the points in Figure 16.<sup>42</sup> The continuous line is a plot of the relationship

$$i = 1 - \exp\left\{-\frac{(\chi_A - \chi_B)^2}{4}\right\} \quad (33)$$

due to Pauling, and is a rather good fit to the experimental data.

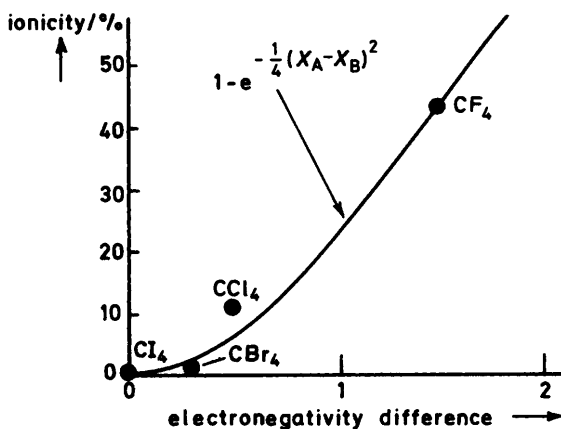


Figure 16 Plot of ionic character of the C–X bond in the tetrahalides as deduced from their quadrupole coupling constants against the C–X electronegativity difference

Chlorine, bromine, and iodine quadrupole resonance frequencies are fairly easy to detect by conventional r.f. oscillator spectrometers, and a wide range of values has been recorded in numerous types of organic and inorganic compound. Such comprehensive data can often be used to infer charge distributions and stereochemistry in a related group of compounds using the simple assumption that if the structure of one member of the series is known, and the quadrupole resonance spectra of most other members are similar, then the stereochemistry of the whole



series is taken to be the same. A different spectral type must then correspond to a different stereochemistry. A recent example occurs in an investigation<sup>70</sup> of Sn<sup>IV</sup> chloride adducts of the type SnCl<sub>4</sub>·2L with an octahedral stereochemistry; a *trans* configuration of the two ligands L should give rise to just one <sup>35</sup>Cl frequency, possibly with small splittings due to crystallographic non-equivalence, whereas a *cis* configuration should give rise to at least two different <sup>35</sup>Cl frequencies, arising from the two different types of chlorine atom (axial and equatorial) which it contains, with frequency differences which are expected to be larger than any crystal effects and possibly a different temperature dependence for each set. Experiment bears out these conclusions although the distinction is not always as clear-cut as these arguments imply; however the results in Table 4 suggest that the Bu<sup>n</sup>CN adduct has a *cis* structure, as is usually found for nitrile adducts, and the tetrahydrothiophene adduct a *trans* structure, in agreement with an analysis of its vibrational spectrum.

**Table 4** <sup>35</sup>Cl quadrupole resonance frequencies (in MHz) in SnCl<sub>4</sub> and two of its adducts at 77 K (average temperature coefficient (kHz K<sup>-1</sup>) in brackets)

SnCl <sub>4</sub>	SnCl <sub>4</sub> ·2Bu <sup>n</sup> CN	SnCl <sub>4</sub> ·2THF
23.720	19.390 (-2.7)	17.42 (-0.8)
24.140	19.535 (-2.7)	17.88 (-1.1)
24.226	19.650 (-1.1)	
24.296	20.285 (-1.2)	

Because of the simplicity of the energy level diagram of spin- $\frac{3}{2}$  nuclei, measurements of the spin-lattice relaxation time of <sup>35</sup>Cl and <sup>79</sup>Br are particularly useful in the interpretation of molecular dynamics in solids. In relaxation recovery experiments, *e.g.* with a simple 90° pulse sequence, they show simple exponential behaviour with a relaxation time,  $T_{1Q}$ , dominated by quadrupole rather than magnetic relaxation. This fact is easy to settle for nuclei with more than one abundant quadrupolar isotope by measuring  $T_{1Q}$  for at least two isotopes; in the former case the  $T_{1Q}$  ratios will be proportional to the ratio of the squares of the nuclear quadrupole coupling constants and in the latter to the ratio of the squares of the nuclear magnetic moments. Quadrupole relaxation, for example, is the dominant mechanism in determining <sup>79</sup>Br spin-lattice relaxation in K<sub>2</sub>PtBr<sub>6</sub> which between 40 and 500 K shows at least three different types of behaviour (Figure 17).<sup>69</sup> At low temperatures, two <sup>79</sup>Br lines are observed with very similar spin-lattice relaxation times closely proportional to  $T^{-2}$ , behaviour predicted when the predominant mechanism arises from fluctuations in the electric field gradient due to lattice modes. Phase transitions are detected at 78, 105, 137, 143, and 169 K, the last producing a spectacular 'cusp' in the temperature variation of  $T_1$  which is typical of 'soft-mode' transitions, in which in this case the frequency of a rotary lattice mode of the PtBr<sub>6</sub><sup>2-</sup> ion drops precipitously from 27 cm<sup>-1</sup> at 300 K to 16 cm<sup>-1</sup> at 170 K. Above 320 K, relaxation is dominated by hindered re-orientation of the PtBr<sub>6</sub><sup>2-</sup> ion, and  $T_{1Q}$  depends exponentially on temperature

<sup>70</sup> P. G. Huggett, R. J. Lynch, T. C. Waddington, and K. Wade, *J. Chem. Soc., Dalton Trans.*, 1980, 1164.

$$T_{1Q} = T_{1Q}^0 \exp\left(\frac{E^*}{RT}\right) \quad (34)$$

typical of thermally activated processes, in this case with an activation energy  $E^*$  of  $28 \text{ kJ mol}^{-1}$

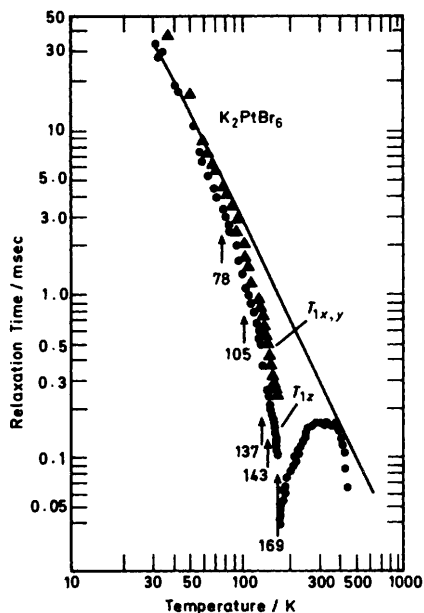


**Figure 17** Temperature variation of the  $^{79}\text{Br}$  spin-lattice relaxation time in  $\text{K}_2\text{PtBr}_6$ . The straight line has a slope of  $-2$

Many of the heavier elements also have quadrupolar nuclei in reasonable abundance, and the study of their quadrupole resonance spectra in organometallic compounds, and metals and alloys, are topics of great current interest; indeed, in the case of some elements, *e.g.* Os, the only ground state magnetic nucleus,  $^{189}\text{Os}$ , is quadrupolar ( $I = \frac{3}{2}$ ), so that quadrupole resonance methods of one kind or another may be necessary for its detection. We conclude this section by giving one example from each of these two groups of materials.

In metals and alloys, the novel electronic feature is the loss of some of the atom's valence electrons to form delocalized orbitals in the conduction band; the calculation of their contribution to the observed quadrupole splittings presents an important theoretical problem, the solution of which would throw light not only on the band structure, but also on the electron distribution over the whole of the metal lattice, both near to and away from the metal ions. There is one important



be overall positive). Conversely an increase in the  $\pi$ -acceptor power of X will reduce the  $3d_{zx}$  and  $3d_{yz}$  populations and so increase the quadrupole coupling constant. So in the series X =  $-\text{SiCl}_3$ ,  $-\text{GeCl}_3$ ,  $-\text{SnCl}_3$ , assuming the same geometry, the  $^{59}\text{Co}$  quadrupole coupling constants at 77 K are 130.7, 162.0 (an average value), and 163.5 MHz (with almost zero asymmetry parameters), demonstrating the greater  $\sigma$ -donor ability of  $-\text{SiCl}_3$ .  $^{55}\text{Mn}$  and  $^{185,187}\text{Re}$  quadrupole resonance has also been studied in a number of their organometallic complexes, and the method is in principle extendable to many other transition metals, over 70% of which have suitable quadrupolar nuclei in reasonable abundance.

*Acknowledgements.* The author would like to thank the many authors and editors of periodicals who have given permission to reproduce some of the figures in this review, a number of contributors to the 8th n.q.r. Symposium (1985) in Darmstadt for preprints of their papers, and Dr. D. E. Ames for a sample of 2-methylquinazolin-4-one.